Trabajo Fin de Grado
Grado en Ingeniería de las Tecnologías Industriales

Oxford Foot Model Kinetic Analysis During the Stance Phase in Gait

Autor: José David Jarmell Carrasco
Tutor: Joaquín Ojeda Granja

Dep. Ingeniería Mecánica y Fabricación
Escuela Técnica Superior de Ingeniería
Universidad de Sevilla

Sevilla, 2016

Oxford Foot Model Kinetic Analysis During the Stance Phase in Gait

Trabajo Fin de Grado
Ingeniería Mecánica y Fabricación

Oxford Foot Model Kinetic Analysis During the Stance Phase in Gait

Autor:
José David Jarmell Carrasco

Tutor:
Joaquín Ojeda Granja
Profesor ayudante doctor

Dep. de Ingeniería Mecánica y Fabricación
Escuela Técnica Superior de Ingeniería
Universidad de Sevilla
Sevilla, 2016

Oxford Foot Model Kinetic Analysis During the Stance Phase in Gait

Trabajo Fin de Grado: Oxford Foot Model Kinetic Analysis During the Stance Phase in Gait

Autor: José David Jarmell Carrasco

Tutor: Joaquín Ojeda Granja

El tribunal nombrado para juzgar el Trabajo arriba indicado, compuesto por los siguientes miembros:

Presidente:

Vocales:

Secretario:

Acuerdan otorgarle la calificación de:

Sevilla, 2016

El Secretario del Tribunal

A mi familia: Isabel, Mitchell y Sara; Pepe y Mari Pepa; Sol y Ethel.

Acknowledgements

I wish to thank Mr. Joaquín Ojeda Granja for the time he has dedicated to me at all times and for introducing me to this exciting and worthwhile field.

Also, special thanks to Mr. Philippe Dixon, for the interest he has put into my work and for unselfishly devoting his time to me.

Lastly, I would like to mention Mr. José Luis Escalona Franco for his patience in explaining the big picture to me, which I was missing and ended up being of great value to my work.

Abstract

The objective in the present paper was to obtain the forces and moments present in the joint formed by the Forefoot and Hindfoot segments in the Oxford Foot Model (OFM) via an inverse kinetic approach.

The starting point of the work is a number of experimental data gathered using a set of retroreflective markers and a stereophotogrammetry camera, as well as the information collected by a Ground Reaction Force Plate (GRF).

With the markers' data, we are able to know the position and orientation at all times of the different segments that comprise the OFM multi-segment model. After that, the velocities and accelerations, both linear and angular, are obtained using the finite difference method for calculating derivatives.

An estimation of the masses, centers of gravity and moments of inertia were needed in order to calculate our desired outcome.

An analysis of the different forces and moments that affect our system was conducted: the gravitational force, the ones derived from the Force Plate and the ones in the inter-segment area were found, as well as the inertial summands of the equations. And so, it was a closed problem that would be resolved using the Newton-Euler equations, the output of which are the three components of the inter-segment forces and moments.

These results were later on compared to those obtained by Dixon et al. (2012), with the main difference between the two studies found in the age group of the subjects employed by each study; in the case of Philippe Dixon, he studied the gait in a set of young, healthy adolescents, while this paper's experimental data is collected using a male adult subject.

The findings were an increase in peak values in the moments and power, with a similar progression in the shape of the three graphs in this study. This was thought to be caused by the increased weight and size of the individual in this study.

Also, an analysis was done to see the relative importance of each of the summands of the equations used, finding that the inertial ones play a negligible role in them, and thus could be not taken into account for further studies, at least when pursuing a first result with less precision required.

Finally, the results could be improved if further information regarding centers of gravity and moments of inertia was available, in stead of having to estimate them using limited information, and if more trials with the same subject and with other subjects of a similar age and weight group in order to eliminate repeatability issues.

Index

Oxford Foot Model Kinetic Analysis During the Stance Phase in Gait

FIGURE INDEX

Oxford Foot Model Kinetic Analysis During the Stance Phase in Gait

TABLE INDEX

Oxford Foot Model Kinetic Analysis During the Stance Phase in Gait

Notation

$\mathbf{A_i}$	Rotation matrix for segment *i*
$\boldsymbol{\omega_i}$	Angular velocity vector for segment *i*, in global coordinate system
$\boldsymbol{\alpha_i}$	Angular acceleration vector for segment *i*, in global coordinate system
$\bar{\boldsymbol{\omega}}_\mathbf{i}$	Angular velocity vector for segment *i*, in local coordinate system
$\bar{\boldsymbol{\alpha}}_\mathbf{i}$	Angular acceleration vector for segment *i*, in local coordinate system
$\mathbf{v_i^O}$	Linear velocity vector of origin point O of segment *i*, in global coordinate system
$\mathbf{a_i^O}$	Linear acceleration vector of origin point O of segment *i*, in global coordinate system
$\mathbf{a_i^G}$	Linear acceleration vector of center of gravity G of segment *i*, in global coordinate system
$\boldsymbol{\theta_i}$	Euler Parameters vector for segment *i*
e0	First Euler Parameter
e1	Second Euler Parameter
e2	Third Euler Parameter
e3	Fourth Euler Parameter
HX	Hallux segment of the model

FF	Forefoot segment of the model
HF	Hindfoot segment of the model

1 INTRODUCTION

Human motion analysis is a very important aspect within mechanics, specially because of the endless possibilities of what can be done with the collected data, such as newer, lighter and more customized prostheses for the limbs in the body or as an aid in clinical decision-making, specially in surgical treatment. However, for it to be applicable, it is important that repeatability and validity of these models is investigated prior to its routinely employment. This probably is one of the most exciting and worthwhile fields at the times we live in.

Kinematic analyses of foot models have been extensively researched, both using mono-segment as well as multi-segment models, gathering data from all sorts of age groups and genders. However, in the case of kinetic analyses, the same cannot be said: although for mono-segment models there are plenty of studies that have been conducted, there is a shortage of kinetic analyses of multi-segment models, so it is this particular area that we intend on shedding some light upon. Also, the existing paper studies young adolescents, and in in this specific one, the focus will be on a healthy adult.

1.1. State of the art

Two of the best, most well-researched kinematic analyses of multi-segment foot models that have been conducted have mainly centered their efforts in the repeatability aspect of the results, (Carson et al., 2001), (Stebbins et al., 2005); more than focusing on the individual findings, they have analyzed the inter and intra-subject deviations that occur in this type of an experiment.

In the former of the two papers, the author explains that there have been several researchers who have described multi-segment foot model's kinematics, although the marking and describing of the segment-embedded axes have varied between each one of them, so comparability is limited and thus a standardized protocol is needed, which requires thorough testing and validation. As a result, the first paper has the goal of developing a multi-segment foot model and measurement protocol applicable to gait and evaluating the reliability of this protocol and model. According to this article, certain patterns and ranges of motion between segments of the foot were detected", and repeatability between days or individuals was "primarily subject to variability of marker placement more than inter-tester variability or skin movement". The Hallux segment presented greater variability than desired due to increased vibrations in the combination of markers used.

In the latter of them, the authors adapt a previously existing foot model to the case of children, which present several challenges, such as a decreased surface area of the foot to place the markers and greater variability in gait. Experimenting with a number of variations to it, they experienced minimal changes in repeatability. Also, since most of the published studies are limited to the stance phase of gait, the author intends on expanding it to the entire gait cycle.

As far as kinetic trials go, the referent in articles in this field is a paper comparing the results obtained via mono-segment and multi-segment models (Dixon et al., 2012). Also, within the multi-segment case, it assesses different "joints" in the Oxford Foot Model (OFM): the Tibia/Hindfoot, as well as the Hindfoot/Forefoot one. In this paper, the author explains differences he expects to encounter with respect to the mono-segment case when trying to analyze the kinetics of a multi-segment foot model, such as a probable reduction of the peak ankle dorsiflexion, since the relative movement of the forefoot and hindfoot are isolated from that of the ankle. Also, a decrease in peak sagittal plane moment and thus power, as the single rigid foot models may overestimate the contribution of the ankle joint. Kinetics play a major role in identifying, evaluating and treating gait abnormalities, for example in the comprehension of ankle kinetics, since this joint provides the main propulsive power in the gait cycle. The third and last expected result would be non-negligible power generation in the Midfoot since muscle and tendon activity are present at this location during gait. They found that there was a great decrease through OFM calculations compared to PIG estimates; not

caused by a decrease in joint moments, but in the angular velocity between tibia and hindfoot.

1.2. Objectives

The main goal in this study is to replicate Phil Dixon's results in his kinetic analysis paper, implementing a code that may be used in the future by our department in this type of problem, and serving as a basis for further codes that estimate the moments we are seeking in a more precise manner. The main difference between the two will be the age group selected by each one of the studies; Phil Dixon worked with young adolescents and in our case it will be a male adult.

A secondary objective here is to evaluate the relevance of each of the summands in the equations used to calculate the inter-segment forces and moments in the multi segment foot model. If any of them are negligible in comparison to the rest, for further studies, there may be an important and acceptable simplification of the calculations involved in this type of analyses.

1.3. Motivation for a multi-segment approach

The foot can be modeled as a single rigid body, with no relative motion between or within its different segments. However, this provides inadequate information when determining treatment specific to the foot.

Kinetic analysis have been mainly conducted in mono-segment foot models, like the PIG model, for example. The problem with these is that the forces involved in gait are unknown unless further segmenting is conducted. This way, it is unclear which parts of the foot suffer more aggressively the inner-foot forces that result from the process of walking.

Mono-segment models are insufficient to reveal intra and inter-segment foot kinematic changes during gait, and thus cannot isolate foot pathologies to a specific joint.

Many multi-segment foot models are being proposed and it is important that the repeatability and reliability of these models be thoroughly investigated before they are routinely used to inform clinical decision-making. The Oxford Foot Model (OFM) is the most widespread model in scientific circles; the problem is that there is only one paper addressing its kinetics, and is not without important limitations.

2 STARTING POINT. EXPERIMENTAL DATA

The Oxford Foot Model (OFM) is composed of three different segments, without any restrictions of movement between them. The first segment, the most distal one from the ankle, is the Hallux segment (HX), which anatomically corresponds to the Hallux toe, limited to the extension of this phalange. The second segment is the Forefoot (FF), which corresponds to the volume surrounding the metatarsal bones in the midfoot. Lastly, the most proximal segment to the ankle is the Hindfoot (HF), which is composed of the volume limited by the Talus and Calcaneus bones.

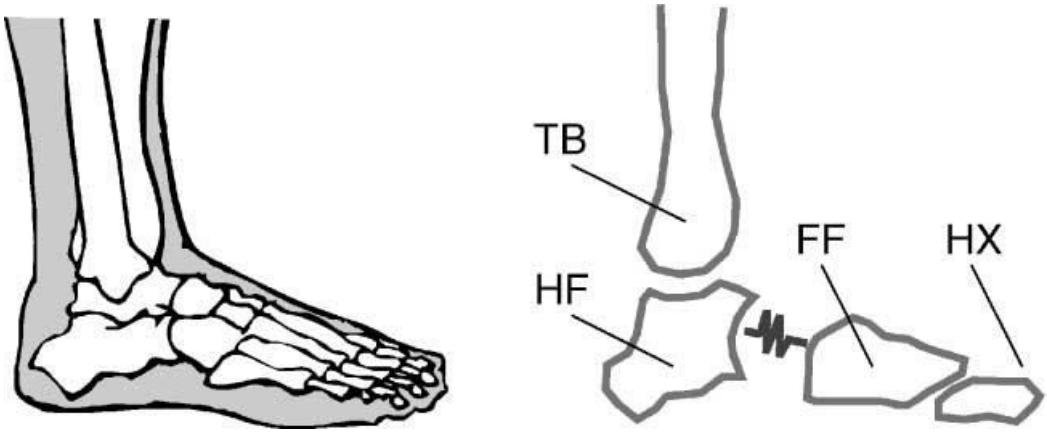

Figure 1, Matching of the Oxford Foot Model's segments to the human foot, (Carson et al., 2001)

Kinematic data was collected through an experimental trial, where the subject was asked to walk in a straight line, stepping over a force plate to gather information including force and moment referred to its center of gravity.

Retroreflective markers where strategically placed on the subject's foot, enabling local coordinate systems to be defined using the positions of multiple of these markers. The axes of these local reference systems for each segment were intended to coincide with the normal vectors to the anatomical sagittal, frontal and transverse planes. The information of their position during the trial was captured using stereophotogrammetry cameras, with a frequency of 100 Hz.

2.1 Retroreflective Markers

The position of the markers where captured in two different stages; the first one, in a static trial, where one allows the software to identify each marker with known positions. More markers than strictly needed are used in order to compensate for deviations in the desired placement. After this stage is complete, some of the redundant markers are removed in order to cause the least interference possible with the movement that we want to analyze.

In the dynamic trail, the markers used for each segment to define the coordinate axes are the following:

Hindfoot

- RHEE (Origin of the HF segment*)
- RCPG

- RLCA

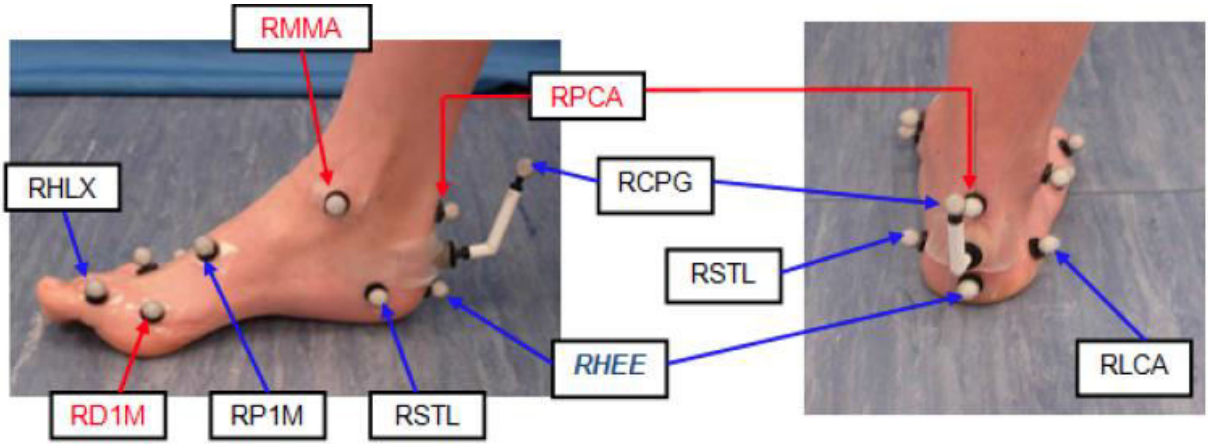

Figure 2, Placement of markers for the experimental trial on the foot, (Vicon Oxford Foot Model 1.4 Release Notes)

Forefoot

- RP1M (Origin of the FF segment*)
- RD5M
- RP5M
- RTOE

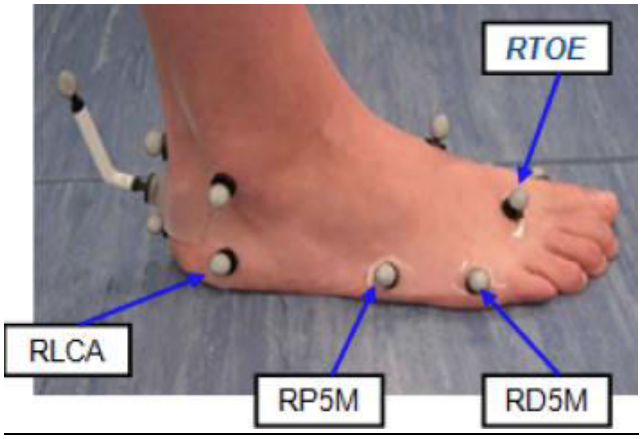

Figure 3, Placement of markers for the experimental trial on the foot, (Vicon Oxford Foot Model 1.4 Release Notes)

Hallux

- RHLX (Origin of the HX segment*)

- RD1M
- Plus, an axis defined for the FF segment.

*The markers used as segment origins were arbitrarily chosen to be those.

2.2 Global Coordinate System

The dynamic trial is conducted aiming for the trajectory followed by the individual to be a straight line and following the *y* global axis, which is parallel to the floor . The *x* global axis is also horizontal and perpendicular to the *y* axis pointing towards the right side of the subject. Finally, axis *z* is vertical and pointing upwards.

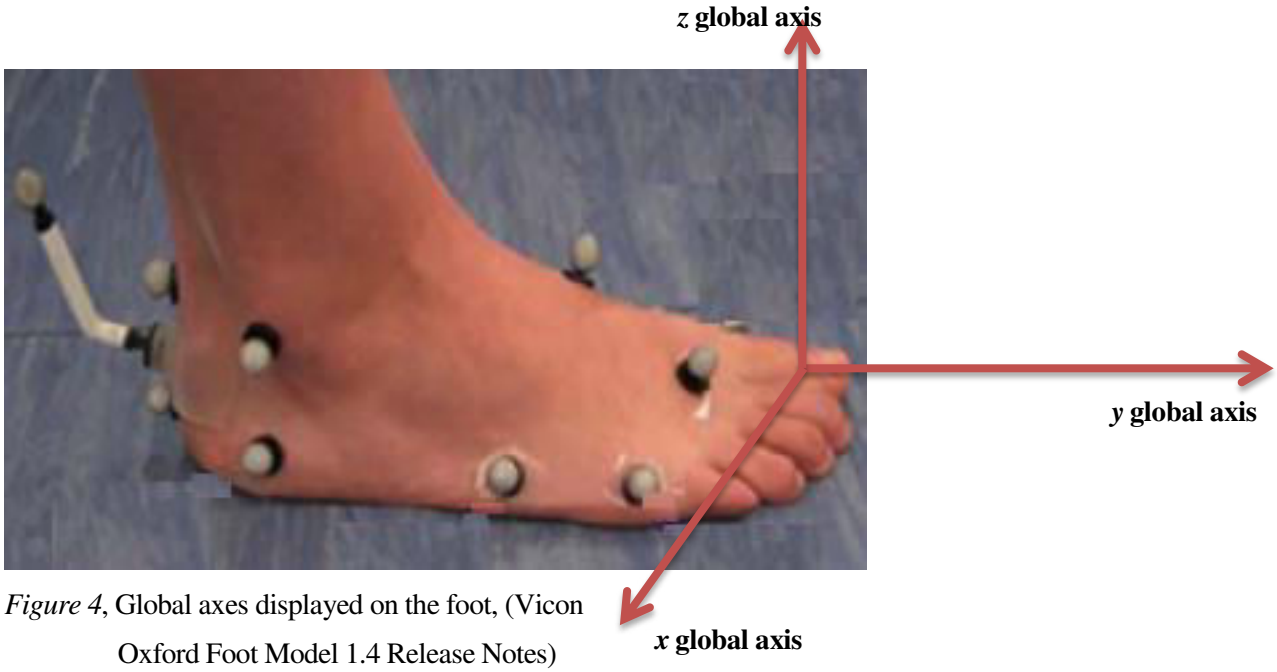

Figure 4, Global axes displayed on the foot, (Vicon Oxford Foot Model 1.4 Release Notes)

2.3 Ground Reaction Force (GRF) Plate

The Ground Reaction Force Plate is located on the floor. The output information it provides is the forces applied to the foot (the opposite of the one it suffers from it) as well as the bending moment exerted towards the foot as a reaction to the balance of forces applied by the foot. These forces and moments are expressed in the global coordinate system, and are refreshed at the same pace as the position of the markers, 100 Hz.

The progression with time of each of the three forces and moments of the force plate have the following graphs as outputs:

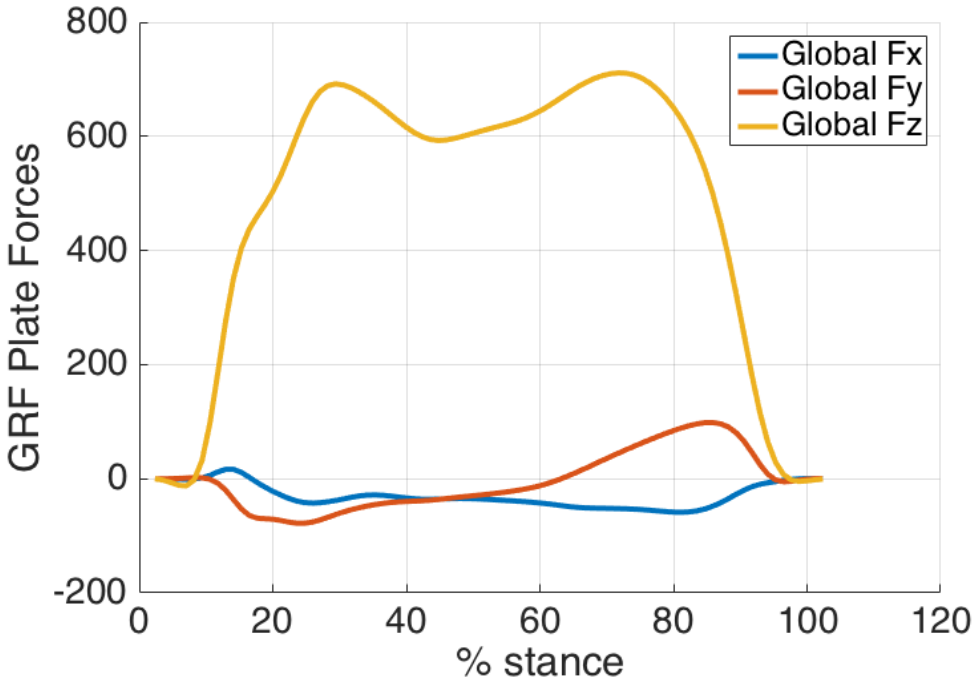

Figure 5, Progression of GRF Forces with time in all three global cartesian axes, expressed in N

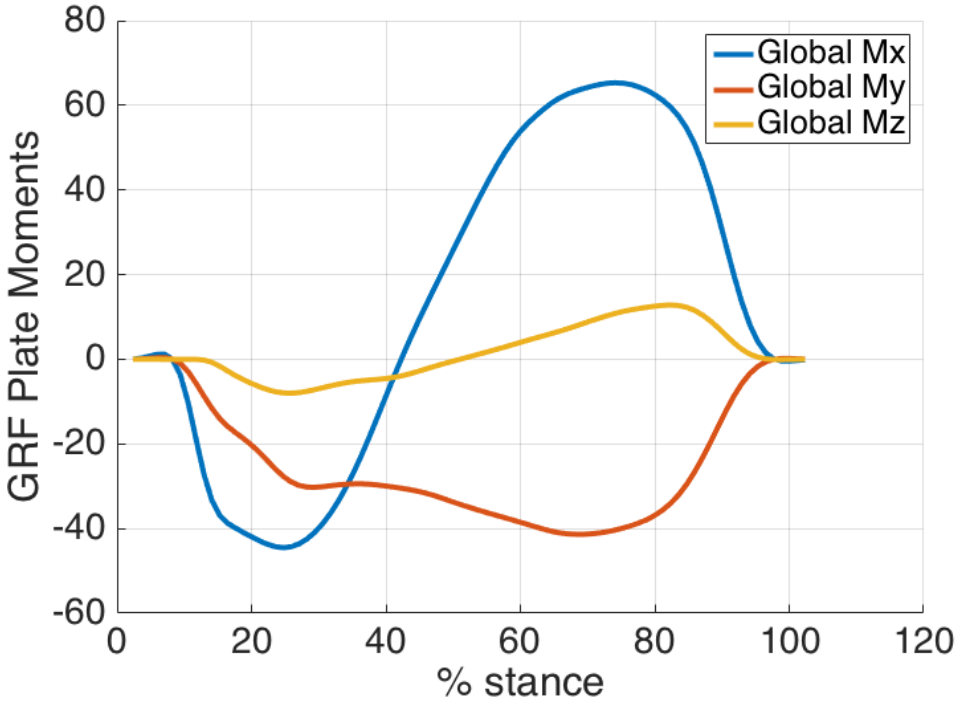

Figure 6, Progression of GRF Moments with time in all three global cartesian axes, expressed in N·m

3 MULTI-SEGMENT BODY

3.1 Segments Origins

When the kinematic analysis is complete, one of the output results we will have will be the position for every instant of the experiment of the origin of the segments. With this information we will be able to calculate the position, velocity and acceleration of any point of their points. The specific markers used as origin of each one have been mentioned in section 2.1.

3.2 Local Coordinate System

In the static trial, for each segment, the *x* axis is perpendicular to the frontal plane of the body and positive being towards the direction of gait; the *y* axis, perpendicular to the sagittal plane of the human body and with positive orientation towards the left foot of the subject; finally, the *z* axis is normal to the transverse plane of the subject's body and with the positive orientation being upwards.

These orientations will coincide with these directions only in the static trail, since all these local coordinate systems are not fixed, as opposed to the global coordinate system.

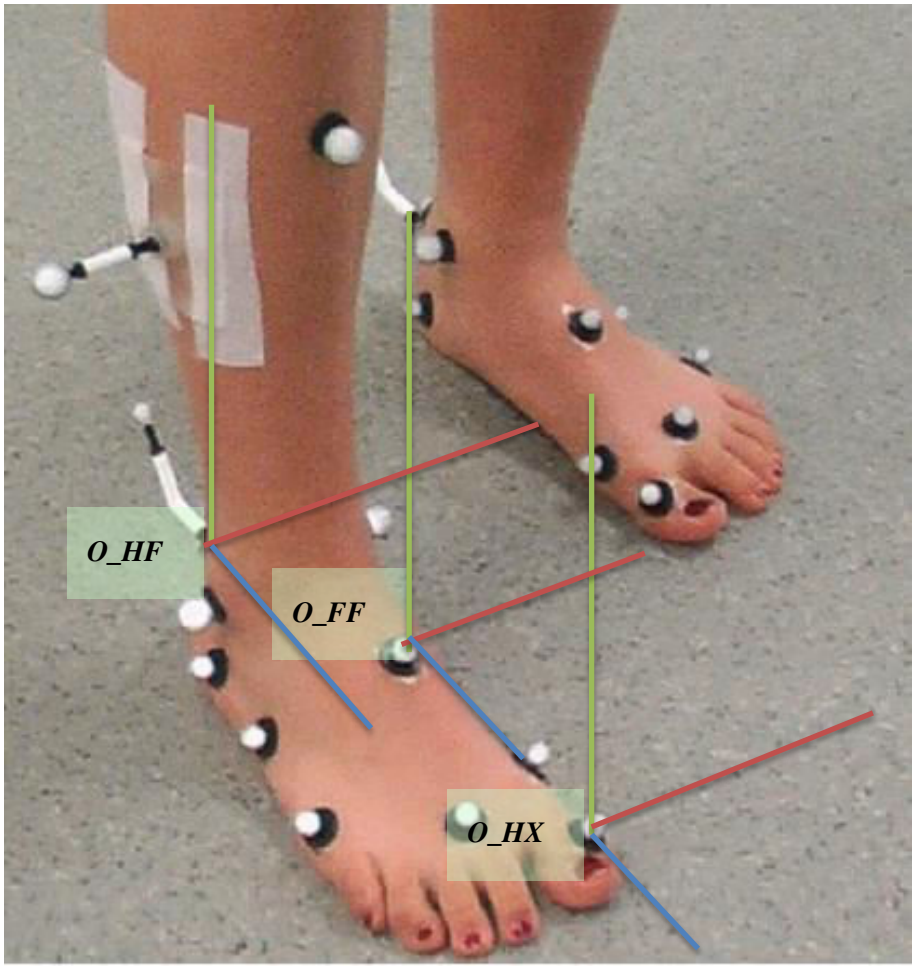

Figure 7, Local cartesian reference systems and markers set as origins for all three segments

Each one of the three green lines correspond to the *z* local axes; the blue lines are the *x* local axes; and the red lines correspond to the *y* local axes. Also, *O_HF*, *O_FF* and *O_HX* refer to the origin of each of these three segments.

3.3 Spatial Orientation. Euler Parameters

This is the third piece of information we need, besides the segments' origins and the ground reaction forces, to be able to obtain the position of any of their points and to conduct the kinetic analysis. With the array of four Euler Parameters of each segment we will be able to build the rotation matrix for every of these parts, which converts any vector expressed in the local reference system to its equivalent in the global reference system. Also, the two matrices needed to calculate the angular velocities and angular accelerations using the first and second time-derivatives of the array of Euler Parameters.

3.4 Estimation of length for each segment

Total length of the foot is approximately 25 cm. Hallux segment length was estimated to be the one of the hallux metatarsal bones of the foot, around 5 cm. The two other segments were set to be half of the remaining length (the total of the foot minus the hallux), 10 cm each.

$$length(HX) = 5\ cm$$

$$length(FF) = 10\ cm$$

$$length(HF) = 10\ cm$$

3.5 Estimation of mass for each segment

Total mass of the foot is approximately 1.37% of the total mass of the body in the case of men (de Leva et al., 1996), which is about 1 kg considering that the subject's mass is 73 kg. The masses of both the Forefoot as well as the Hindfoot were arbitrarily set to half the total mass of the foot (Dixon et al., 2012). The Hallux segment was estimated to be one-fifth of the mass of the other two segments.

$$mass(HX) = 0.1\ kg$$

$$mass(FF) = 0.5\ kg$$

$$mass(HF) = 0.5\ kg$$

3.6 Distribution of GRF

The distribution of the GRF amongst the three segments is very hard to estimate, given that the only information we receive from it is the total force and moment that it applies towards the foot in its center of gravity. We do, however, know where each marker is in relation to the plates' cog; this way, if we had a device that measured relative pressures over the GRF plate, the accuracy in this sense would be much greater.

Since we don't know where this force is being applied, it is convenient to look for a situation where an approximation may be reasonable. We observe that once Heel Rise (HR) occurs, the Hindfoot isn't in contact with the force plate (Dixon et al., 2012); from this point on, only the Forefoot and the Hallux are.

Also, since the surface of contact between the Hallux segment and the floor is much smaller than that of the Forefoot with the floor, we'll assume that from HR until takeoff (the first moment at which there stops being any contact at all between the floor and the foot), the only part affected by the force plate will be the Forefoot.

HR has been observed to occur a little bit before the point when the marker in the heel, RHEE, exceeds its vertical position in a 10% with respect to that of the static trial (Dixon et al., 2012).

Since this is the interval (between HR until takeoff) where we have the most information on where the GRF is being applied, it will be the only part where we'll conduct the analysis.

3.7 Hallux Segment Removal

Given that:

- We have simplified the problem assuming the GRF does not have an effect over the Hallux segment
- The Hallux's mass and inertia are much smaller than those of the other two segments
- As we will be able to verify in the *"Results"* section, the predominant force, much greater that the inertial summands, is the GRF

we will reduce the problem by removing the Hallux segment from the equation. Barely any difference at all can be observed by making this change; however, it is of great help in means of facilitating the understanding of the problem when attempting to solve it.

3.8 Estimation of cog of each segment

Because of the simplifications we have made, only the center of gravity of the Forefoot will be needed. Taking the RP1M marker on the Forefoot as the origin of this segment, the local vector (that is, in the FF Coordinate System) connecting it to the FF's cog, was estimated to be (units in meters):

$$\overline{\mathbf{cog}}_{\mathbf{FF}} = [-0.02 \;\; 0.02 \;\; -0.03]'$$

3.9 Inertia Tensors for each segment

The Inertia Tensor was decided to be calculated in the local coordinate system for each segment, due to the fact that the moment equations would be solved in the same reference system.

There is available information as to how to conduct the calculations for the case of mono-segment foot models. However, for multi-segment models there isn't much information at all.

The adopted solution was to begin calculations as if the model were the first, and then to divide the inertia into all the segments.

For the mono-segment model, the moment of inertia about a given axis is:

$$I = (M \cdot \bar{m}) \cdot (l \cdot \bar{r})^2 \quad (1)$$

where M is the total mass of the subject, $\bar{m}$ is the mean percentage of (mono) segment mass, l is the (mono) segment length and $\bar{r}$ is the mean radius of gyration about the corresponding axis. So using the following parameters:

M	73 kg
$\bar{m}$	1.37%
l	0.25 m
$\bar{r}$ (de Leva et al., 1996.)	25.7% for *x*-axis
	24.5% for *y*-axis
	12.4% for *z*-axis

Table 1, Parameters needed to calculate the Moments of Inertia for the mono-segment foot model

As a result, the moment of inertia about each axis is the following:

Ix	0.0048 kg·m^2
Iy	0.0044 kg·m^2
Iz	0.0011 kg·m^2

Table 2, Moments of Inertia about each of the three axes for the mono-segment foot model

Now, for further segmenting the foot model, the decision was to use a scaling factor (sf) for each segment depending on its moment of inertia, as follows:

$$sf = \frac{segment\ mass \cdot segment\ length^2}{foot\ mass \cdot foot\ length^2} \quad (2)$$

sf (HX)	0.0034
sf (FF)	0.0739
sf (HF)	0.0739

Table 3, Scaling factors for the three segments

So, as a result, for each segment, the moments of inertia will be calculated as:

$$I_k(segment) = sf \cdot I_k(total) \quad (3)$$

where *k* refers to the axis about which we want to calculate the given moment.

With regard to the inertia tensor, as previously happened with the center of gravity, the only one we are truly interested in is the Forefoot's:

$$\mathbf{I}\ (FF) = 10^{-3} \cdot \begin{bmatrix} 0.3575 & 0 & 0 \\ 0 & 0.3249 & 0 \\ 0 & 0 & 0.0832 \end{bmatrix}$$

4 KINEMATICS

4.1 Rotation Matrix for each segment

Since we will be using Euler Parameters for spatial orientation, we will need the expression of the Rotation Matrix using these parameters, which has the following structure:

$$\mathbf{A}\ (\text{segment}_i, \mathrm{t}_k) = \begin{bmatrix} 1-2\cdot e_2^2-2\cdot e_3^2 & 2\cdot(e_1\cdot e_2-e_0\cdot e_3) & 2\cdot(e_1\cdot e_3+e_0\cdot e_2) \\ 2\cdot(e_1\cdot e_2+e_0\cdot e_3) & 1-2\cdot e_1^2-2\cdot e_3^2 & 2\cdot(e_2\cdot e_3-e_0\cdot e_1) \\ 2\cdot(e_1\cdot e_3-e_0\cdot e_2) & 2\cdot(e_2\cdot e_3+e_0\cdot e_1) & 1-2\cdot e_1^2-2\cdot e_2^2 \end{bmatrix} \quad (4)$$

(Nikravesh, P. E., 1988)

where segment_i refers to any of the two segments after the Hallux segment simplification (FF, HF) and t_k refers to any *k* instant of time between Heel Rise and takeoff.

This rotation matrix will allow us to obtain any vector that is in expressed in the local coordinate system of any of the segments in the global coordinate system simply by pre-multiplying it by this matrix; similarly, the opposite will be possible by simply using the inverse of this rotation matrix in the same fashion.

Lastly, to change the expression of any given vector between two local reference systems, we will only have to pre-multiply it by two consecutive rotation matrices: first, the inverted matrix of the new local system and second, the one of the previous system.

4.2 Calculation of $\boldsymbol{\omega_i}$, $\boldsymbol{\alpha_i}$ $\boldsymbol{\bar{\omega}_i}$, $\boldsymbol{\bar{\alpha}_i}$, $\boldsymbol{v_i^O}$, $\boldsymbol{a_i^O}$

For the calculation of $\boldsymbol{\omega_i}$, $\boldsymbol{\alpha_i}$, $\boldsymbol{\bar{\omega}_i}$ and $\boldsymbol{\bar{\alpha}_i}$, we will use one of two matrices to relate angular velocity or angular acceleration to the first or second time-derivatives of the Euler Parameters' array, which are:

$$\mathbf{L}\ (segment_i, t_k) = \begin{bmatrix} -e_1 & e_0 & e_3 & -e_2 \\ -e_2 & -e_3 & e_0 & e_1 \\ -e_3 & e_2 & -e_1 & e_0 \end{bmatrix} \quad (5)$$

$$\mathbf{G}\ (segment_i, t_k) = \begin{bmatrix} -e_1 & e_0 & -e_3 & e_2 \\ -e_2 & e_3 & e_0 & -e_1 \\ -e_3 & -e_2 & e_1 & e_0 \end{bmatrix} \quad (6)$$

where **L** and **G** are the initials of Local, Global to relate angular velocity and acceleration in local or global reference systems to the Euler Parameter's time-derivatives, using the following expressions:

$$\boldsymbol{\omega_i} = 2 \cdot \mathbf{G_i} \cdot \dot{\boldsymbol{\theta}}_\mathbf{i} \tag{7}$$

$$\bar{\boldsymbol{\omega}}_\mathbf{i} = 2 \cdot \mathbf{L_i} \cdot \dot{\boldsymbol{\theta}}_\mathbf{i} \tag{8}$$

$$\boldsymbol{\alpha_i} = 2 \cdot \mathbf{G_i} \cdot \ddot{\boldsymbol{\theta}}_\mathbf{i} \tag{9}$$

$$\bar{\boldsymbol{\alpha}}_\mathbf{i} = 2 \cdot \mathbf{L_i} \cdot \ddot{\boldsymbol{\theta}}_\mathbf{i} \tag{10}$$

For the two other variables, $\mathbf{v_i^O}$ and $\mathbf{a_i^O}$, all we have to do is calculate the first and second time-derivatives, respectively, of the position vector of each segment's origin.

4.3 Calculation of a_i^G

Once we have calculated all of the previous variables, obtaining $\mathbf{a_i^G}$ is just a matter of employing the following expression to relate them:

$$\mathbf{a_i^G} = \mathbf{a_i^O} + \boldsymbol{\alpha_i} \wedge \overline{\mathbf{OG}}_\mathbf{i} + \boldsymbol{\omega_i} \wedge (\boldsymbol{\omega_i} \wedge \overline{\mathbf{OG}}_\mathbf{i}) \tag{11}$$

where $\overline{\mathbf{OG}}$ can be expressed as:

$$\overline{\mathbf{OG}}_\mathbf{i} = \mathbf{A_i} \cdot \overline{\mathbf{cog}}_\mathbf{i} \tag{12}$$

where $\overline{\mathbf{cog}}_\mathbf{i}$ is the position vector of the center of gravity of segment *i* with respect to the origin of that same segment, in its local coordinate system.

5 INVERSE KINETICS

5.1 Actions involved

In general, for any given segment, the forces that will play a role will be the following:

- Gravitational forces
- Inter-segment forces
- GRF forces

Similarly, the moments will include:

- Inter-segment moments
- Inter-segment force-derived moments
- GRF moments
- GRF force derived moments

5.2 Formulation of the problem

The force balance equation will be expressed using the global reference system, whereas the moment balance equation will be expressed in the Forefoot's local reference system.

The reasons for the second decision are the following:

- In the local coordinate system, since it is fixed with respect to the segment, the inertia tensor will be constant in time.
- In the local coordinate system, since it is fixed with respect to the segment, the inertia tensor will only have elements in its diagonal.

For every segment we will be using two three-dimensional vector equations, one as a force balance ($\sum_k \mathbf{F_k} = m_i \cdot \mathbf{a_i^G}$) and the other as a moment balance ($\sum_k \mathbf{M_k} = \mathbf{I_i} \cdot \boldsymbol{\alpha_i}$), which will be calculated in the Forefoot's center of gravity; However, since the Hallux segment was removed for simplicity reasons, we will only need the equations of the Forefoot segment:

$$\mathbf{F_{HF-FF}} + \mathbf{F_{grav}} + \mathbf{F_{GRF}} = m_{FF} \cdot \mathbf{a_{FF}^G} \tag{13}$$

$$\mathbf{M_{HF-FF}} + \mathbf{F_{HF-FF}} \wedge \mathbf{r_{int-cdgFF}} + \mathbf{M_{GRF}} + \mathbf{F_{GRF}} \wedge \mathbf{r_{GRF-cdgFF}} - \boldsymbol{\omega_{FF}} \wedge (\mathbf{I_{FF}} \cdot \boldsymbol{\omega_{FF}}) = \mathbf{I_{FF}} \cdot \boldsymbol{\alpha_{FF}} \tag{14}$$

where $r_{int-cdgFF}$ is the position vector that goes connects the interface (the "joint" between two segments) between Hindfoot and Forefoot and the center of gravity of the later and $r_{GRF-cdgFF}$ is the position vector that connects the center of gravity of the force plate to the center of gravity of the Forefoot.

Our two only unknowns will be the inter-segment forces and moments between the Hindfoot and the Forefoot ($\mathbf{F_{HF-FF}}$ and $\mathbf{M_{HF-FF}}$), since:

- $\mathbf{F_{grav}} = [0 \;\; 0 \;\; -m_{FF} \cdot g]'$, constant and known
- $\mathbf{F_{GRF}}$ is a piece of information derived from the force plate
- m_{FF} was estimated in section 3
- $\mathbf{a_{FF}^{G}}$ is known as a result of the kinematic calculations explained in section 5
- $\mathbf{r_{int-cdgFF}}$ is derived from the estimation of the Forefoot's segment length, and assuming its center of gravity is at the mid-point of the longitudinal *x* axis
- $\mathbf{M_{GRF}}$ is a piece of information derived from the force plate
- $\mathbf{r_{GRF-cdgFF}}$ is a variable that is completely defined by knowing the position of the GRF's center of gravity (which is stored as a variable as a result of the kinematic analysis) and the position of the Forefoot's center of gravity.
- $\boldsymbol{\omega_{FF}}$ was calculated in section 5
- $\mathbf{I_{FF}}$ was calculated in section 3
- $\boldsymbol{\alpha_{FF}}$ was calculated in section 5

Also, the summand $-\boldsymbol{\omega_{FF}} \wedge (\mathbf{I_{FF}} \cdot \boldsymbol{\omega_{FF}})$ is part of the second equation because it will be calculated using local coordinates as opposed to a global coordinate system, like is the case in the first equation.

6 RESULTS

The reference systems used for each one of the results are the following: as far as the MidFoot Internal Moments go, the Hindfoot's local Cartesian system was used; in the case of the angles between the Hindfoot and the Forefoot, relative degrees were employed.

On the left of the following pairs of images we will be able to observe the results obtained for the present study and, on the left, those presented by Philippe Dixon in his 2012 paper. Vertical dashed lines in his results represents the timing of heel rise (HR). Shaded grey area represents standard deviation of OFM data.

6.1 MidFoot Angles

Although obtaining kinematic results is not the main focus of the work here presented, it is also needed in order to conduct future comparisons, since the kinematic results that follow in section 7.2 do depend greatly on them.

Heel Rise occurs at approximately 43% of the stance phase. After this point, all three angles increase until 80% of stance is reached, after which there is a sharp decline, generally concluding around the zero-degree point.

Dorsiflexion and abduction present the greatest of the peak values, with suppination reaching only around half of the magnitude formed in the other two planes.

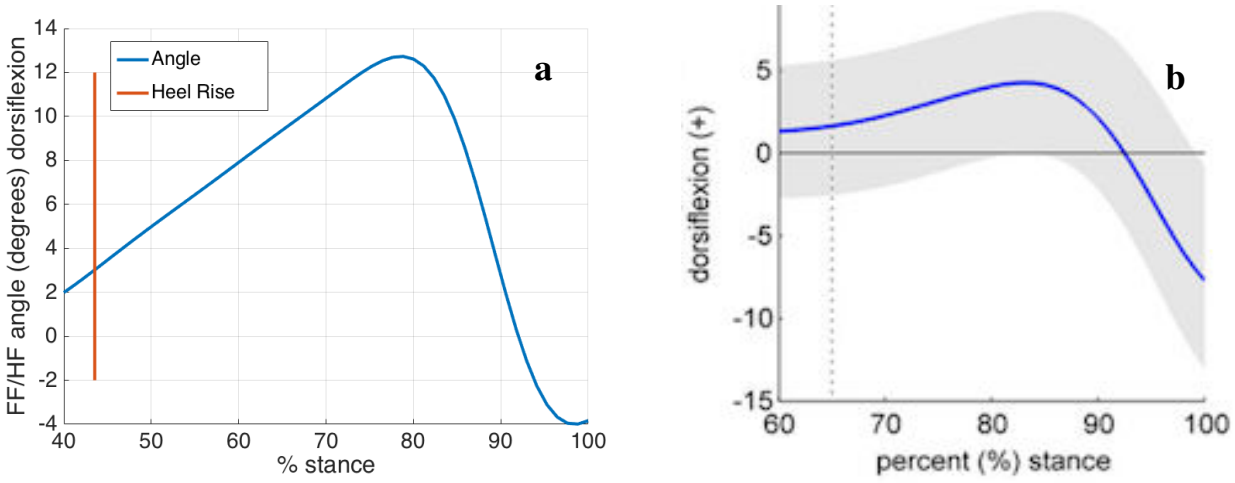

Figure 8, change of dorsiflexion angles with time in the FF/HF joint, (a) in present study and (b) in Philippe Dixon's

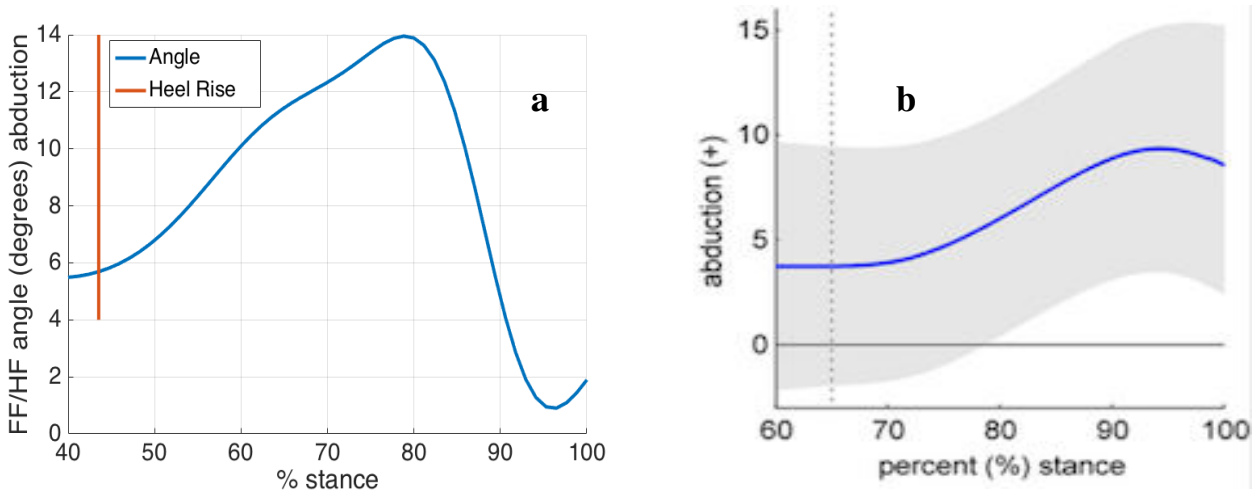

Figure 9, change of abduction angles with time in the FF/HF joint, (a) in present study and (b) in Philippe Dixon's

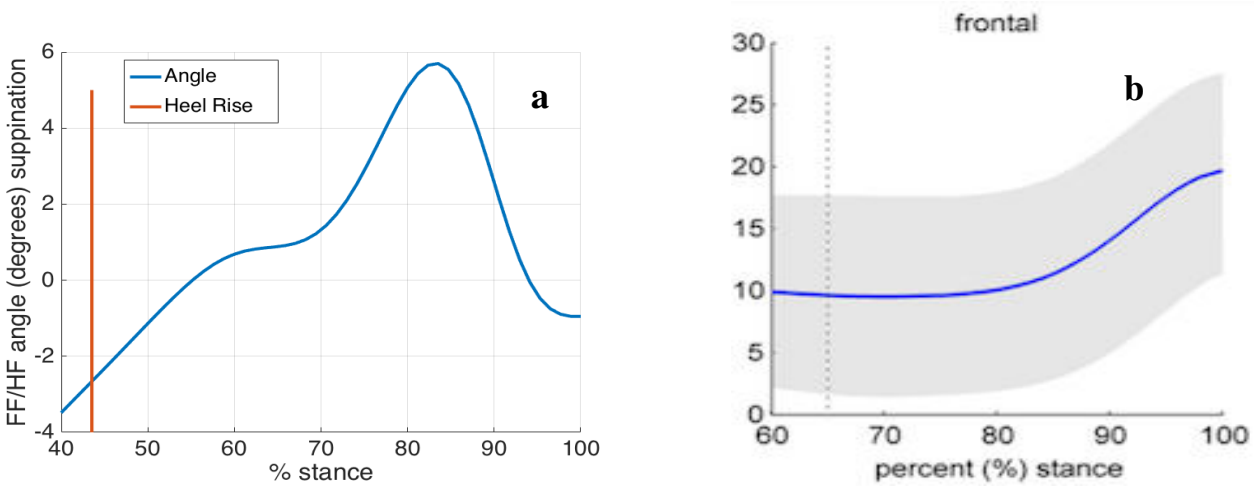

Figure 10, change of suppination angles with time in the FF/HF joint, (a) in present study and (b) in Philippe Dixon's

6.2 MidFoot Moments

This is the main focus of the present study. General shapes of the curves were found to be very similar to those presented by Dixon et al. (2012), although peak values for the two first figures (plantarflexion and pronation) were much greater than in the aforementioned case, between a five and a ten-fold increase. Conversely, in the third figure, peak value is close to Dixon's, as is the overall shape if we only take into account the portion starting at 60% of stance phase, which is approximately the value at which Heel Rise occurs in the case of his study.

The most reasonable explanation for such great of a difference in magnitude is the nature of the subjects; in Dixon et al. (2012), individuals were young adolescents (ages around 14 years of age), with a body weight of approximately 53 kg, whereas in the present study, the subject is a 33 year old adult, with a weight of 73 kg.

The general progression of the plantarflexion moment is a start in the negative values before Heel Rise, with a change in sign from this point on. This change is very intuitive, given that from a simple observation of the foot's motion one can clearly see this inversion in the bend.

Peak value is found between 70 and 80% of stance phase, reaching around 1,000 N·mm. At 100% of this phase, after the toe's takeoff, there is no more bending moment in this direction of the foot.

In the case of the pronation, just like in the findings of Dixon et al. (2012), the initial slope (at around Heel Rise) is of a much lesser value than in the previous case. Similarly, peak magnitude only reaches around 650 N·mm, and at around the same point, approximately at 75% of stance. Even though this value is also much greater than in the case of reference, it is true that the proportion between the two respective figures in both trials is constant, which would seem reasonable if the sole difference between the studies were the subjects used.

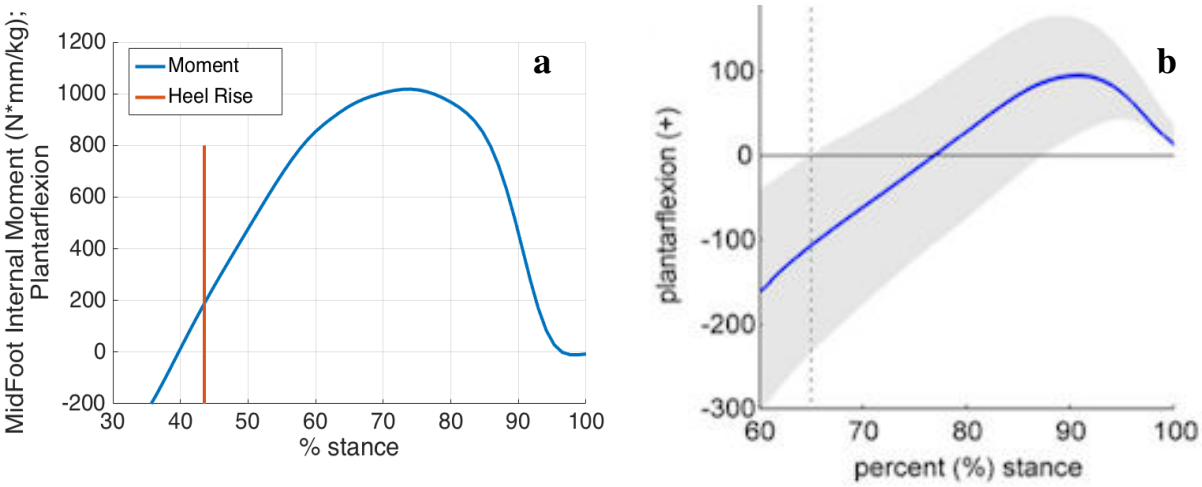

Figure 11, change of plantarflexion internal moments with time in the FF/HF joint, (a) in present study and (b) in Philippe Dixon's

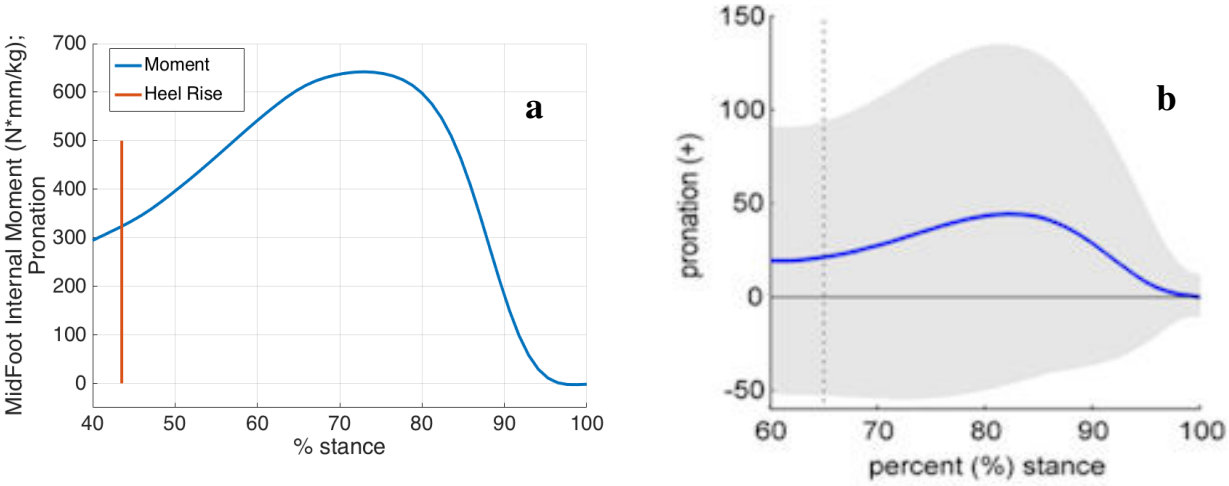

Figure 12, change of pronation internal moments with time in the FF/HF joint, (a) in present study and (b) in Philippe Dixon's

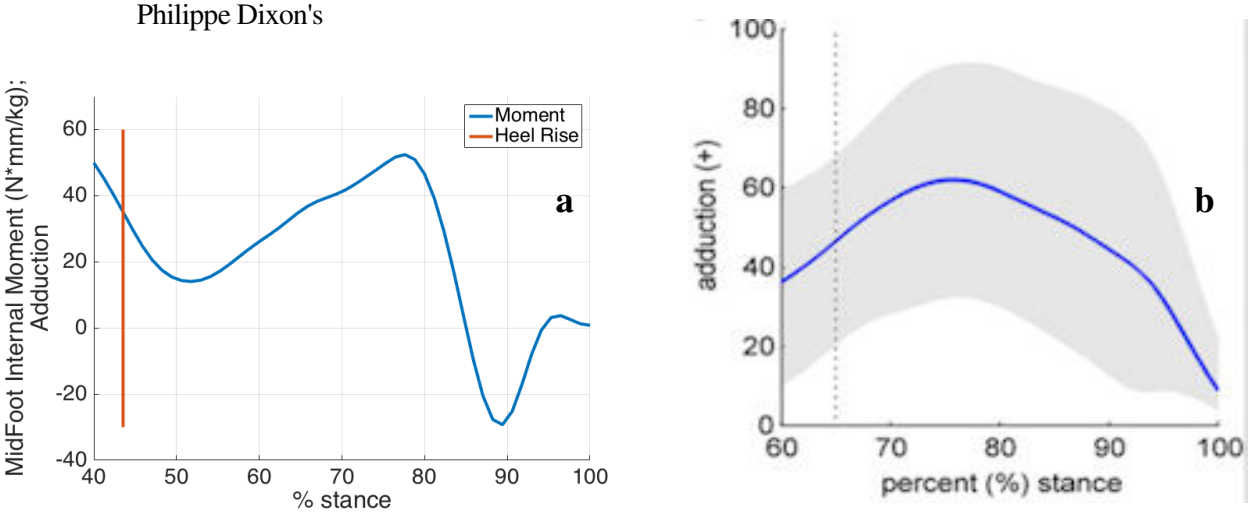

Figure 13, change of adduction internal moments with time in the FF/HF joint, (a) in present study and (b) in Philippe Dixon's

6.3 MidFoot Power Generation

Given the difference between the moments results presented by Dixon et al. (2012), and those in this document, one would also expect power to be between five and ten times greater than in the former case; however, it is only between two and four times greater. If this were true, it would mean that angular velocity in the adult subject is slower than in the young adolescents.

As far as the shape goes, it is identical to its analogous in Dixon's paper: peak value reached at around 85 to 90% of the stance phase, and a power of around zero up until rather advanced stages in this phase, finishing at zero a little bit before the takeoff of the Hallux.

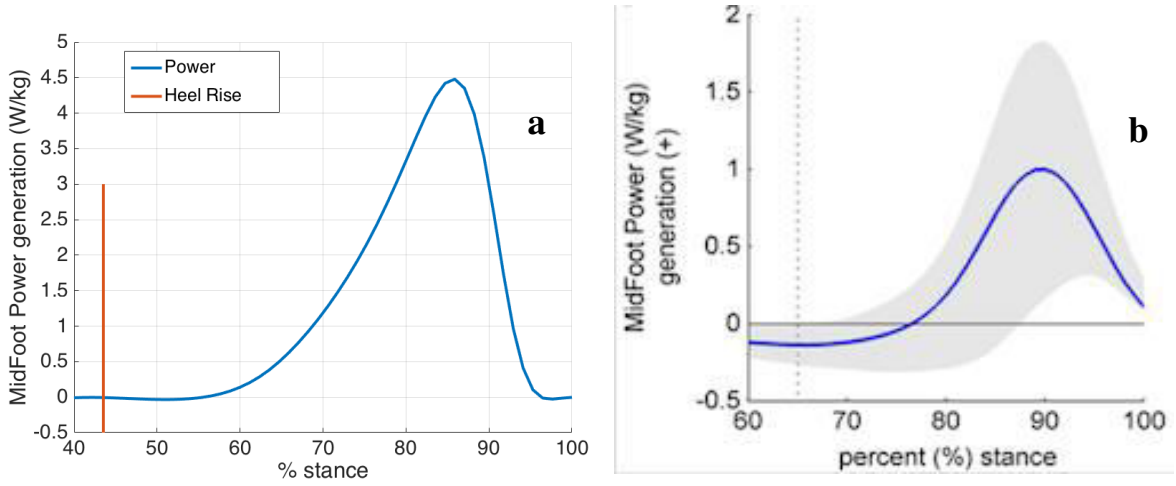

Figure 14, change of power with time in the FF/HF joint, (a) in present study and (b) in Philippe Dixon's

6.4 Relative Importance of each summand of the equation

Throughout the following figures, which represent the summands of the moment's equation in all three axis, we can observe the negligible inertial contribution of the dynamic equations to the overall result. The predominant factor in them is the ground reaction force, in the case of the force equation, and ground reaction moment and moment derived from force in the moments equation.

In the moments equation (which are the results presented in these three figures), there is a smaller but very significant contribution of the moment caused by the midfoot's inner forces, which are no more than a mere result of the balance between forces, where the ground reaction force is predominant.

$$\mathbf{F_{HF-FF}} + \mathbf{F_{grav}} + \mathbf{F_{GRF}} = m_{FF} \cdot \mathbf{a_{FF}^{G}} \tag{13}$$

$$\mathbf{M_{HF-FF}} + \mathbf{F_{HF-FF}} \wedge \mathbf{r_{int-cdgFF}} + \mathbf{M_{GRF}} + \mathbf{F_{GRF}} \wedge \mathbf{r_{GRF-cdgFF}} - \boldsymbol{\omega}_{\mathbf{FF}} \wedge (\mathbf{I_{FF}} \cdot \boldsymbol{\omega}_{\mathbf{FF}}) = \mathbf{I_{FF}} \cdot \boldsymbol{\alpha}_{\mathbf{FF}} \tag{14}$$

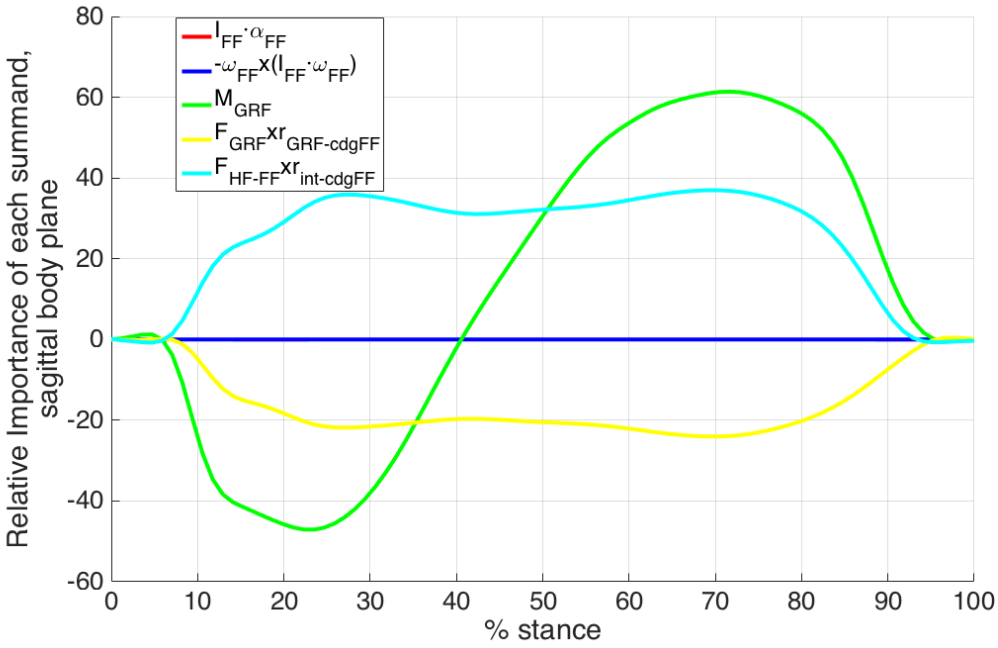

Figure 15, change of relevance of each summand in the moment's equation in the sagittal plane of the body with time

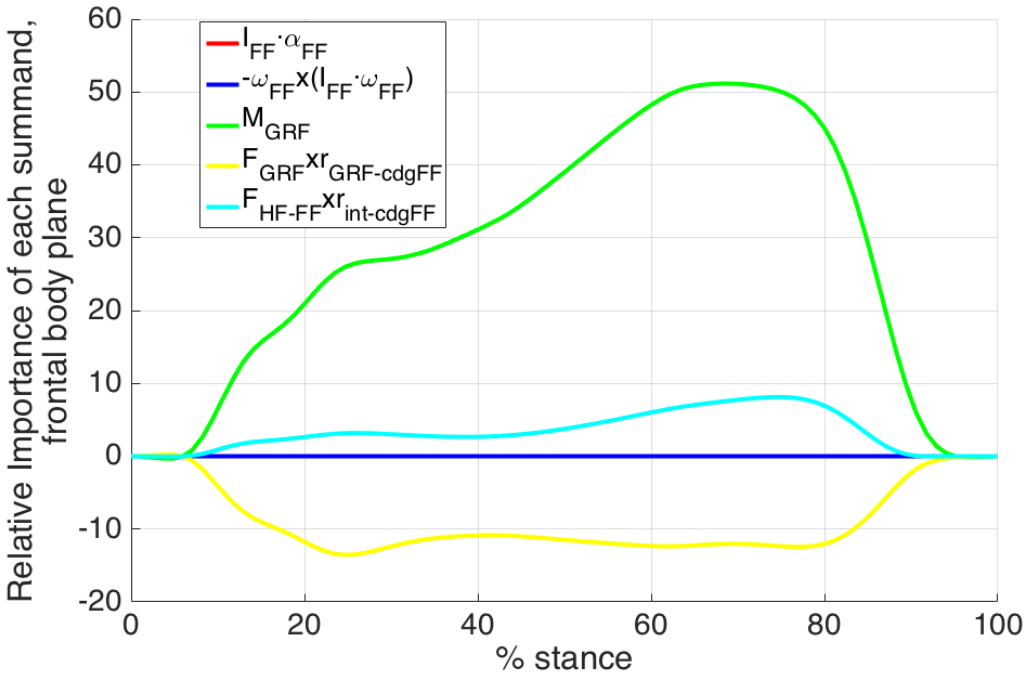

Figure 16, change of relevance of each summand in the moment's equation in the frontal plane of the body with time

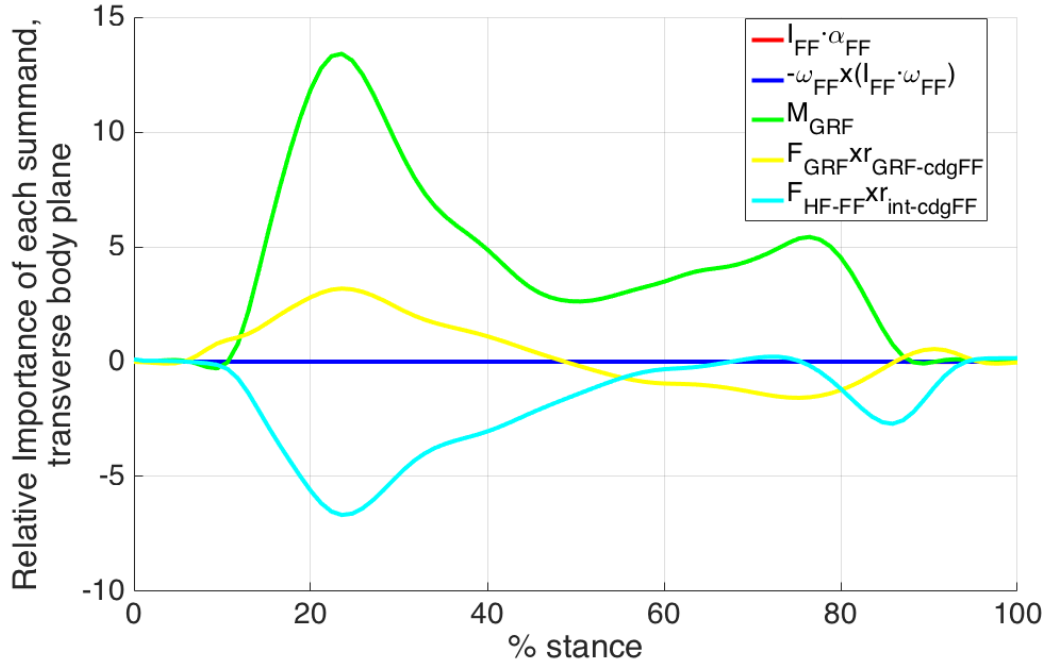

Figure 17, change of relevance of each summand in the moment's equation in the transverse plane of the body with time

7 CONCLUSIONS

The path followed for the present work was the following:

First, we gathered the data from the changing position of the retroreflective markers and the forces and moments from the GRF Plate. With the data from the positions we obtained the linear accelerations of the chosen origins of the segments, as well as the Euler Parameters for them, which enabled us to calculate the angular velocities and accelerations for all three segments, as well as the linear accelerations for the centers of gravity of the bodies.

Secondly, we simplified the problem assuming that the Hallux segment has a negligible contribution to the system and that the information gathered from the GRF Plate only has an effect (once Heel Rise occurs) over the Forefoot.

Thirdly, we introduced the information in the equations; we knew the accelerations and almost all the present forces and wanted to obtain as an output the only one we didn't know, which is the force exerted by the Hindfoot upon the Forefoot. Different approaches were followed to obtain the remaining parameters; the total mass of the foot was extracted from the de Leva article, and its distribution between all three segments was estimated; total length of the foot was measured and distribution, once again estimated; total radius of gyration about each axis was obtained from the de Leva article. Then, total moments of inertia were calculated using these radii. The distribution of these moments between all three segments was calculated from there.

Finally, the angles, moments and power in the HF-FF joint were plotted for the whole stance phase, along with the relevance of each summand of the equation.

After analyzing these results and comparing them to those presented by Dixon et al. (2012), the following conclusions can be extracted:

- In the present study, an adult subject was in charge of gathering the data; a 40% increase in his weight with respect to the young adolescents in the aforementioned paper could explain the difference in two of the three magnitudes of the moments, with the shape being very similar in all cases.
- Given that this experiment was only conducted on one subject, and only in one occasion, it is possible that some peculiarities out of the ordinary in gait were captured and thus further differentiation in the moments' magnitudes have been made evident, through a prior difference in the relative angles between the segments.
- As a non-linear problem, the possibility of small errors in marker placement (specially as the subject was the one placing his owns markers) may have lead to a big distortion in relative angles between the different segments.
- Lack of information about the GRF distribution has forced to making certain simplifications which may not be ideal; using more advanced technology, such as a device informing of pressure distribution, would aid in this sense. Probably the Hallux segment is more important than presented in this paper, as for instance, in the last fraction of the stance phase, it is the only segment in contact with

the floor; however, since it had previously been eliminated, the forces gathered by the force plate were directly applied to the Forefoot.

- A better method for estimating both, the centers of gravity, as well as the moments of inertia of each segment (there was adequate information only for the mono-segment case) would be very useful.

8 REFERENCES

Carson, M. C., Harrington, M. E., Thompson, N., O'Connor, J. J., Theologis, T. N., 2001. Kinematic analysis of a multi-segment foot model for research and clinical applications: a repeatability analysis. Journal of Biomechanics 34 (10), 1299-1307

de Leva, P., 1996. Adjustments to Zatsiorsky-Seluyanov's segment inertia parameters. Journal of Biomechanics 29 (9), 1223-1230

Dixon, P. C., Böhm, H., Döderlein, L., 2012. Ankle and midfoot kinetics during normal gait: A multi-segment approach. Journal of Biomechanics 45 (6), 1011-1016

Nikravesh, P. E., 1988. Computer aided analysis of mechanical systems

Stebbins, J., Harrington, M., Thompson, N., Zavatsky, A., Theologis, T., 2006. Repeatability of a model for measuring multi-segment foot kinematics in children. Gait Posture 23 (4) 401-410

Vicon Motion Systems Limited. Oxford Foot Model 1.4 Release Notes June 2012

ANNEX A: KINETIC ANALYSIS MAIN CODE

```
%%%%%%%%%%%%%%%%%%%%%%%%%%%%%%%%%%%
%%KINETIC ANALYSIS OFM FOOT MODEL%%
%%%%%%%%%%%%%%%%%%%%%%%%%%%%%%%%%%%

Dt=Options.VideoFrameRate^(-1);
dim=size(position,1);
t=[1:dim]*Dt;
g=9.81;


% Euler Parameters, Segment Origins Positions and their first and second
time-derivatives

EulerParam=zeros(dim,4);

EulerParam(:,1:4)=position(:,11:14);

dtEulerParam=zeros(dim,4);
ddtEulerParam=zeros(dim,4);


R=zeros(dim,3);

R(:,1:3)=position(:,8:10);

dtR=zeros(dim,3);
ddtR=zeros(dim,3);


for i=2:(dim-1)

    dtEulerParam(i,:)=(EulerParam(i+1,:)-EulerParam(i-1,:))/(2*Dt);
    dtR(i,:)=(R(i+1,:)-R(i-1,:))/(2*Dt);

end

 dtEulerParam(dim,:)=dtEulerParam(dim-1,:);
 dtR(dim,:)=dtR(dim-1,:);

for i=2:(dim-1)

    ddtEulerParam(i,:)=(dtEulerParam(i+1,:)-dtEulerParam(i-1,:))/(2*Dt);
    ddtR(i,:)=(dtR(i+1,:)-dtR(i-1,:))/(2*Dt);

end

ddtEulerParam(dim,:)=ddtEulerParam(dim-1,:);
ddtR(dim,:)=ddtR(dim-1,:);


%Angular velocities and accelerations in local and global coordinate systems


for i=1:dim
```

```
    L=matrizL(EulerParam(i,1:4));
    w_loc(i,1:3)=2*L*dtEulerParam(i,1:4)';
    alfa_loc(i,1:3)=2*L*ddtEulerParam(i,1:4)';


    G=matrizG(EulerParam(i,1:4));
    w_glob(i,1:3)=2*G*dtEulerParam(i,1:4)';
    alfa_glob(i,1:3)=2*G*ddtEulerParam(i,1:4)';


end


%Acceleration of the Forefoot's center of gravity

%Center of gravity vector

cdg_FF=[-0.02 0.02 -0.03]';


for i=1:dim


A_FF=matrizA_EulerParam(EulerParam(i,1:4));
aG_FF(i,:)=ddtR(i,1:3)+cross(alfa_glob(i,1:3)',(A_FF*cdg_FF))'+cross(w_glob(i
,1:3)',cross(w_glob(i,1:3)',(A_FF*cdg_FF)))';

end

% Segments masses

v=[1 1 1];
Id=diag(v);
Z=zeros(1,3);
ZZ=zeros(3,3);

m_HX=100*10^(-3);
m_FF=500*10^(-3);
m_HF=500*10^(-3);

mTot=m_HX+m_FF+m_HF;

% Relative radius of gyration (to the mono-segment length)


r_x=25.7/100;
r_y=24.5/100;
r_z=12.4/100;

long_pie=25.81/100;

% Moments of inertia for the mono-segment case

Ix=mTot*(r_x*long_pie)^2;
Iy=mTot*(r_y*long_pie)^2;
Iz=mTot*(r_z*long_pie)^2;

% Segment lengths

l_HX=0.05;
l_FF=(long_pie-l_HX)/2;
l_HF=l_FF;
```

```
% Inertia Tensors and scaling factors (fe)

fe_FF=m_FF*l_FF^2/(mTot*long_pie^2);
fe_HX=m_HX*l_HX^2/(mTot*long_pie^2);
fe_HF=m_HF*l_HF^2/(mTot*long_pie^2);

Ix_FF=fe_FF*Ix;
Iy_FF=fe_FF*Iy;
Iz_FF=fe_FF*Iz;

I_FF= [Ix_FF 0 0; 0 Iy_FF 0; 0 0 Iz_FF];

% Ground Reaction Forces

GRF_FF=GRF(:,1:6); %glob

% Kinetic Resolution

F_grav=zeros(3,1);
F_grav(3)=-m_FF*g;


for j=1:dim

    A_FF=matrizA_EulerParam(EulerParam(j,1:4));
    A_HF=matrizA_EulerParam(position(j,18:21));


    %% Forces Equation

    Fplaca=GRF(j,1:3)';


    F_HFFF_glob=m_FF*aG_FF(j,:)'-F_grav-Fplaca;

    F_HFFF(:,j)=F_HFFF_glob;


    %% Moments Equation

    acv=-cross(w_loc(j,1:3),(I_FF*w_loc(j,1:3)')');
    r_GRFcdg=(R(j,1:3)'+A_FF*cdg_FF)-(AMTI.pos(:,1:3)'
    r_int_cdg=[l_FF/2 0 0]';
    Mplaca=A_FF^(-1)*GRF(j,4:6)';


    M_HFFF_locFF(:,j)=I_FF*alfa_loc(j,1:3)'-acv-Mplaca-A_FF^(-
1)*(cross(Fplaca,r_GRFcdg))-A_FF^(-1)*(cross(F_HFFF_glob,A_FF*r_int_cdg));
    M_HFFF_loc(:,j)=A_HF^(-1)*A_FF*M_HFFF_locFF(:,j);

    summand1(:,j)=A_HF^(-1)*A_FF*I_FF*alfa_loc(j,1:3)';
    summand2(:,j)=-A_HF^(-1)*A_FF*acv;
    summand3(:,j)=-A_HF^(-1)*A_FF*Mplaca;
    summand4(:,j)=-A_HF^(-1)*(cross(Fplaca,r_GRFcdg));
    summand5(:,j)=-A_HF^(-1)*(cross(F_HFFF_glob,A_FF*r_int_cdg));


end

land=1;
```

```
while abs(GRF_FF(land,3))<1

    land=land+1;

end

land=land-1;

i=1;

while MARKERS.RHEE(i,3)<1.1*35.63*10^(-3) % 35.63 mm is the vertical (z)
coordinate of the RHEE marker in the static trial

    i=i+1;

end

HR=i-1;


lift=10;

while abs(GRF_FF(lift,3))>1

    lift=lift+1;

end

masa_persona=73;

for k=1:dim

    Pot(k)=w_loc(k,1:3)*M_HFFF_locFF(1:3,k);

end


M_HFFF_loc=M_HFFF_loc*1000/masa_persona;
M_HFFF_loc=M_HFFF_loc(:,land:lift);


summand1=summand1(:,land:lift);
summand2=summand2(:,land:lift);
summand3=summand3(:,land:lift);
summand4=summand4(:,land:lift);
summand5=summand5(:,land:lift);


Pot=Pot/masa_persona;
Pot=Pot(land:lift);

tt=[land-2:lift-2]*100/(lift-land);

x=[HR*100/(lift-land) HR*100/(lift-land)];
y1=[-600 800];
y2=[0 500];
y3=[-30 60];
y4=[-0.5 3];
y5=[-2 12];
y6=[-4 5];
y7=[4 14];
```

```
figure(1)
set(gca,'FontSize',28)
hold on
graph1=plot(tt,M_HFFF_loc(2,:),x,y1);
set(graph1,'LineWidth',4)
xlabel('% stance')
ylabel({'MidFoot Internal Moment (N*mm/kg);', 'Plantarflexion'})
legend('Moment','Heel Rise')
axis([30 100 -200 1200])
grid


figure(2)
set(gca,'FontSize',28)
hold on
graph2=plot(tt,M_HFFF_loc(1,:),x,y2);
set(graph2,'LineWidth',4)
xlabel('% stance')
ylabel({'MidFoot Internal Moment (N*mm/kg);', 'Pronation'})
legend('Moment','Heel Rise')
axis([40 100 -50 700])
grid


figure(3)
set(gca,'FontSize',28)
hold on
graph3=plot(tt,M_HFFF_loc(3,:),x,y3);
set(graph3,'LineWidth',4)
xlabel('% stance')
ylabel({'MidFoot Internal Moment (N*mm/kg);', 'Adduction'})
legend('Moment','Heel Rise')
axis([40 100 -40 70])
grid


figure(4)
set(gca,'FontSize',28)
hold on
graph4=plot(tt,Pot,x,y4);
set(graph4,'LineWidth',4)
xlabel('% stance')
ylabel('MidFoot Power generation (W/kg)')
legend('Power','Heel Rise')
axis([40 100 -0.5 5])
grid


Angle2=DATA.JointAngle(:,2,2);
Angle1=DATA.JointAngle(:,1,2);
Angle3=DATA.JointAngle(:,3,2);

Angle2=Angle2(land:lift);
Angle1=Angle1(land:lift);
Angle3=Angle3(land:lift);


figure(5)
set(gca,'FontSize',28)
hold on
graph5=plot(tt,-Angle2,x,y5);
set(graph5,'LineWidth',4)
xlabel('% stance')
ylabel('FF/HF angle (degrees) dorsiflexion')
```

```
legend('Angle','Heel Rise')
axis([40 100 -4 14])
grid


figure(6)
set(gca,'FontSize',28)
hold on
graph6=plot(tt,Angle1,x,y6);
set(graph6,'LineWidth',4)
xlabel('% stance')
ylabel('FF/HF angle (degrees) suppination')
legend('Angle','Heel Rise')
axis([40 100 -4 6])
grid


figure(7)
set(gca,'FontSize',28)
hold on
graph7=plot(tt,-Angle3,x,y7);
set(graph7,'LineWidth',4)
xlabel('% stance')
ylabel('FF/HF angle (degrees) abduction')
legend('Angle','Heel Rise')
axis([40 100 0 14])
grid

figure(8)
set(gca,'FontSize',26)
hold on
graph8=plot(tt,summand1(2,:),'r',tt,summand2(2,:),'b',tt,summand3(2,:),'g',tt
,summand4(2,:),'y',tt,summand5(2,:),'c');
set(graph8,'LineWidth',4)
xlabel('% stance')
ylabel({'Relative Importance of each summand,', 'sagittal body plane'})
legend('I_{FF}·\alpha_{FF}','-
\omega_{FF}x(I_{FF}·\omega_{FF})','M_{GRF}','F_{GRF}xr_{GRF-cdgFF}','F_{HF-
FF}xr_{int-cdgFF}')
axis([0 100 -60 80])
grid

figure(9)
set(gca,'FontSize',28)
hold on
graph9=plot(tt,summand1(1,:),'r',tt,summand2(1,:),'b',tt,summand3(1,:),'g',tt
,summand4(1,:),'y',tt,summand5(1,:),'c');
set(graph9,'LineWidth',4)
xlabel('% stance')
ylabel({'Relative Importance of each summand,', 'frontal body plane'})
legend('I_{FF}·\alpha_{FF}','-
\omega_{FF}x(I_{FF}·\omega_{FF})','M_{GRF}','F_{GRF}xr_{GRF-cdgFF}','F_{HF-
FF}xr_{int-cdgFF}')
axis([0 100 -20 60])
grid

figure(10)
set(gca,'FontSize',28)
hold on
graph10=plot(tt,summand1(3,:),'r',tt,summand2(3,:),'b',tt,summand3(3,:),'g',t
t,summand4(3,:),'y',tt,summand5(3,:),'c');
set(graph10,'LineWidth',4)
xlabel('% stance')
ylabel({'Relative Importance of each summand,', 'transverse body plane'})
legend('I_{FF}·\alpha_{FF}','-
\omega_{FF}x(I_{FF}·\omega_{FF})','M_{GRF}','F_{GRF}xr_{GRF-cdgFF}','F_{HF-
```

```
FF}xr_{int-cdgFF}')
axis([0 100 -10 15])
grid

figure(11)
set(gca,'FontSize',28)
hold on
graph11=plot(tt,GRF_FF(land:lift,1:3));
set(graph11,'LineWidth',4)
xlabel('% stance')
ylabel('GRF Plate Forces')
legend('Global Fx','Global Fy','Global Fz')
grid

figure(12)
set(gca,'FontSize',28)
hold on
graph12=plot(tt,GRF_FF(land:lift,4:6));
set(graph12,'LineWidth',4)
xlabel('% stance')
ylabel('GRF Plate Moments')
legend('Global Mx','Global My','Global Mz')
grid
```

ANNEX B: ROTATION MATRIX CODE

```
function A = matrizA_EulerParam (p)

e0=p(1);
e1=p(2);
e2=p(3);
e3=p(4);

A=[1-2*e2^2-2*e3^2  2*(e1*e2-e0*e3)  2*(e1*e3+e0*e2);

   2*(e1*e2+e0*e3)  1-2*e1^2-2*e3^2  2*(e2*e3-e0*e1);

   2*(e1*e3-e0*e2)  2*(e2*e3+e0*e1)  1-2*e1^2-2*e2^2];
```

ANÁLISIS CINÉTICO DEL MODELO OXFORD DEL PIE:

RESUMEN

JOSÉ DAVID JARMELL CARRASCO

Grado En Tecnología En Tecnologías Industriales

1. KEYWORDS

Oxford Foot Model, Multi-Segment foot, Kinematics, Kinetics, Hindfoot, Forefoot, Hallux, Inverse dynamics, Gait analysis.

2. SUMMARY

The objective in the present paper was to obtain the forces and moments present in the joint formed by the Forefoot and Hindfoot segments in the Oxford Foot Model (OFM) via an inverse kinetic approach.

The starting point of the work is a number of experimental data gathered using a set of retroreflective markers and a stereophotogrammetry camera, as well as the information collected by a Ground Reaction Force Plate (GRF).

With the markers' data, we are able to know the position and orientation at all times of the different segments that comprise the OFM multi-segment model. After that, the velocities and accelerations, both linear and angular, are obtained using the finite difference method for calculating derivatives.

An estimation of the masses, centers of gravity and moments of inertia were needed in order to calculate our desired outcome.

An analysis of the different forces and moments that affect our system was conducted: the gravitational force, the ones derived from the Force Plate and the ones in the inter-segment area were found, as well as the inertial summands of the equations. And so, it was a closed problem that would be resolved using the Newton-Euler equations, the output of which are the three components of the inter-segment forces and moments.

These results were later on compared to those obtained by Dixon et al. (2012), with the main difference between the two studies found in the age group of the subjects employed by each study; in the case of Philippe Dixon, he studied the gait in a set of young, healthy adolescents, while this paper's experimental data is collected using a male adult subject.

The findings were an increase in peak values in the moments and power, with a similar progression in the shape of the three graphs in this study. This was thought to be caused by the increased weight and size of the individual in this study.

Also, an analysis was done to see the relative importance of each of the summands of the equations used, finding that the inertial ones play a negligible role in them, and thus could be not taken into account for further studies, at least when pursuing a first result with less precision required.

Finally, the results could be improved if further information regarding centers of gravity and moments of inertia was available, in stead of having to estimate them using limited information, and if more trials with the same subject and with other subjects of a similar age and weight group in order to eliminate repeatability issues.

Human motion analysis is a very important aspect within mechanics, specially because of the endless possibilities of what can be done with the collected data, such as newer, lighter and more customized prostheses for the limbs in the body or as an aid in clinical decision-

making, specially in surgical treatment. However, for it to be applicable, it is important that repeatability and validity of these models is investigated prior to its routinely employment. This probably is one of the most exciting and worthwhile fields at the times we live in.

Kinematic analyses of foot models have been extensively researched, both using mono-segment as well as multi-segment models, gathering data from all sorts of age groups and genders. However, in the case of kinetic analyses, the same cannot be said: although for mono-segment models there are plenty of studies that have been conducted, there is a shortage of kinetic analyses of multi-segment models, so it is this particular area that we intend on shedding some light upon. Also, the existing paper studies young adolescents, and in in this specific one, the focus will be on a healthy adult.

State of the art

Two of the best, most well-researched kinematic analyses of multi-segment foot models that have been conducted have mainly centered their efforts in the repeatability aspect of the results, (Carson et al., 2001), (Stebbins et al., 2005); more than focusing on the individual findings, they have analyzed the inter and intra-subject deviations that occur in this type of an experiment.

In the former of the two papers, the author explains that there have been several researchers who have described multi-segment foot model's kinematics, although the marking and describing of the segment-embedded axes have varied between each one of them, so comparability is limited and thus a standardized protocol is needed, which requires thorough testing and validation. As a result, the first paper has the goal of developing a multi-segment foot model and measurement protocol applicable to gait and evaluating the reliability of this protocol and model. According to this article, certain patterns and ranges of motion between segments of the foot were detected", and repeatability between days or individuals was "primarily subject to variability of marker placement more than inter-tester variability or skin movement". The Hallux segment presented greater variability than desired due to increased vibrations in the combination of markers used.

In the latter of them, the authors adapt a previously existing foot model to the case of children, which present several challenges, such as a decreased surface area of the foot to place the markers and greater variability in gait. Experimenting with a number of variations to it, they experienced minimal changes in repeatability. Also, since most of the published studies are limited to the stance phase of gait, the author intends on expanding it to the entire gait cycle.

As far as kinetic trials go, the referent in articles in this field is a paper comparing the results obtained via mono-segment and multi-segment models (Dixon et al., 2012). Also, within the multi-segment case, it assesses different "joints" in the Oxford Foot Model (OFM): the Tibia/Hindfoot, as well as the Hindfoot/Forefoot one. In this paper, the author explains differences he expects to encounter with respect to the mono-segment case when trying to analyze the kinetics of a multi-segment foot model, such as a probable reduction of the peak ankle dorsiflexion, since the relative movement of the forefoot and hindfoot are isolated from that of the ankle. Also, a decrease in peak sagittal plane moment and thus power, as the single rigid foot models may overestimate the contribution of the ankle joint. Kinetics play a major

role in identifying, evaluating and treating gait abnormalities, for example in the comprehension of ankle kinetics, since this joint provides the main propulsive power in the gait cycle. The third and last expected result would be non-negligible power generation in the Midfoot since muscle and tendon activity are present at this location during gait. They found that there was a great decrease through OFM calculations compared to PIG estimates; not caused by a decrease in joint moments, but in the angular velocity between tibia and hindfoot.

Objectives

The main goal in this study is to replicate Phil Dixon's results in his kinetic analysis paper, implementing a code that may be used in the future by our department in this type of problem, and serving as a basis for further codes that estimate the moments we are seeking in a more precise manner. The main difference between the two will be the age group selected by each one of the studies; Phil Dixon worked with young adolescents and in our case it will be a male adult.

A secondary objective here is to evaluate the relevance of each of the summands in the equations used to calculate the inter-segment forces and moments in the multi segment foot model. If any of them are negligible in comparison to the rest, for further studies, there may be an important and acceptable simplification of the calculations involved in this type of analyses.

Motivation for a multi-segment approach

The foot can be modeled as a single rigid body, with no relative motion between or within its different segments. However, this provides inadequate information when determining treatment specific to the foot.

Kinetic analysis have been mainly conducted in mono-segment foot models, like the PIG model, for example. The problem with these is that the forces involved in gait are unknown unless further segmenting is conducted. This way, it is unclear which parts of the foot suffer more aggressively the inner-foot forces that result from the process of walking.

Mono-segment models are insufficient to reveal intra and inter-segment foot kinematic changes during gait, and thus cannot isolate foot pathologies to a specific joint.

Many multi-segment foot models are being proposed and it is important that the repeatability and reliability of these models be thoroughly investigated before they are routinely used to inform clinical decision-making. The Oxford Foot Model (OFM) is the most widespread model in scientific circles; the problem is that there is only one paper addressing its kinetics, and is not without important limitations.

Experimental Data

The Oxford Foot Model (OFM) is composed of three different segments, without any restrictions of movement between them. The first segment, the most distal one from the ankle, is the Hallux segment (HX), which anatomically corresponds to the Hallux toe, limited to the extension of this phalange. The second segment is the Forefoot (FF), which corresponds to the

volume surrounding the metatarsal bones in the midfoot. Lastly, the most proximal segment to the ankle is the Hindfoot (HF), which is composed of the volume limited by the Talus and Calcaneus bones.

Kinematic data was collected through an experimental trial, where the subject was asked to walk in a straight line, stepping over a force plate to gather information including force and moment referred to its center of gravity.

Retroreflective markers where strategically placed on the subject's foot, enabling local coordinate systems to be defined using the positions of multiple of these markers. The axes of these local reference systems for each segment were intended to coincide with the normal vectors to the anatomical sagittal, frontal and transverse planes. The information of their position during the trial was captured using stereophotogrammetry cameras, with a frequency of 100 Hz.

Retroreflective Markers

The position of the markers where captured in two different stages; the first one, in a static trial, where one allows the software to identify each marker with known positions. More markers than strictly needed are used in order to compensate for deviations in the desired placement. After this stage is complete, some of the redundant markers are removed in order to cause the least interference possible with the movement that we want to analyze.

Global Coordinate System

The dynamic trial is conducted aiming for the trajectory followed by the individual to be a straight line and following the *y* global axis, which is parallel to the floor . The *x* global axis is also horizontal and perpendicular to the *y* axis pointing towards the right side of the subject. Finally, axis *z* is vertical and pointing upwards.

Ground Reaction Force (GRF) Plate

The Ground Reaction Force Plate is located on the floor. The output information it provides is the forces applied to the foot (the opposite of the one it suffers from it) as well as the bending moment exerted towards the foot as a reaction to the balance of forces applied by the foot. These forces and moments are expressed in the global coordinate system, and are refreshed at the same pace as the position of the markers, 100 Hz.

Local Coordinate System

In the static trial, for each segment, the *x* axis is perpendicular to the frontal plane of the body and positive being towards the direction of gait; the *y* axis, perpendicular to the sagittal plane of the human body and with positive orientation towards the left foot of the subject; finally, the *z* axis is normal to the transverse plane of the subject's body and with the positive orientation being upwards.

These orientations will coincide with these directions only in the static trail, since all these local coordinate systems are not fixed, as opposed to the global coordinate system.

Spatial Orientation. Euler Parameters

This is the third piece of information we need, besides the segments' origins and the ground reaction forces, to be able to obtain the position of any of their points and to conduct the kinetic analysis. With the array of four Euler Parameters of each segment we will be able to build the rotation matrix for every of these parts, which converts any vector expressed in the local reference system to its equivalent in the global reference system. Also, the two matrices needed to calculate the angular velocities and angular accelerations using the first and second time-derivatives of the array of Euler Parameters.

Estimation of length for each segment

Total length of the foot is approximately 25 cm. Hallux segment length was estimated to be the one of the hallux metatarsal bones of the foot, around 5 cm. The two other segments were set to be half of the remaining length (the total of the foot minus the hallux), 10 cm each.

Estimation of mass for each segment

Total mass of the foot is approximately 1.37% of the total mass of the body in the case of men (de Leva et al., 1996), which is about 1 kg considering that the subject's mass is 73 kg. The masses of both the Forefoot as well as the Hindfoot were arbitrarily set to half the total mass of the foot (Dixon et al., 2012). The Hallux segment was estimated to be one-fifth of the mass of the other two segments.

Distribution of GRF

The distribution of the GRF amongst the three segments is very hard to estimate, given that the only information we receive from it is the total force and moment that it applies towards the foot in its center of gravity. We do, however, know where each marker is in relation to the plates' cog; this way, if we had a device that measured relative pressures over the GRF plate, the accuracy in this sense would be much greater.

Since we don't know where this force is being applied, it is convenient to look for a situation where an approximation may be reasonable. We observe that once Heel Rise (HR) occurs, the Hindfoot isn't in contact with the force plate (Dixon et al., 2012); from this point on, only the Forefoot and the Hallux are.

Also, since the surface of contact between the Hallux segment and the floor is much smaller than that of the Forefoot with the floor, we'll assume that from HR until takeoff (the first moment at which there stops being any contact at all between the floor and the foot), the only part affected by the force plate will be the Forefoot.

HR has been observed to occur a little bit before the point when the marker in the heel, RHEE, exceeds its vertical position in a 10% with respect to that of the static trial (Dixon et al., 2012).

Since this is the interval (between HR until takeoff) where we have the most information on where the GRF is being applied, it will be the only part where we'll conduct the analysis.

Hallux Segment Removal

Given that:

- We have simplified the problem assuming the GRF does not have an effect over the Hallux segment
- The Hallux's mass and inertia are much smaller than those of the other two segments
- As we will be able to verify in the *"Results"* section, the predominant force, much greater that the inertial summands, is the GRF

we will reduce the problem by removing the Hallux segment from the equation. Barely any difference at all can be observed by making this change; however, it is of great help in means of facilitating the understanding of the problem when attempting to solve it.

Estimation of cog of each segment

Because of the simplifications we have made, only the center of gravity of the Forefoot will be needed. Taking the RP1M marker on the Forefoot as the origin of this segment, the local vector (that is, in the FF Coordinate System) connecting it to the FF's cog, was estimated to be (units in meters):

$$\overline{\mathbf{cog}}_{\mathbf{FF}} = [-0.02 \;\; 0.02 \;\; -0.03]'$$

Inertia Tensors for each segment

The Inertia Tensor was decided to be calculated in the local coordinate system for each segment, due to the fact that the moment equations would be solved in the same reference system.

There is available information as to how to conduct the calculations for the case of mono-segment foot models. However, for multi-segment models there isn't much information at all.

The adopted solution was to begin calculations as if the model were the first, and then to divide the inertia into all the segments.

For the mono-segment model, the moment of inertia about a given axis is:

$$I = (M \cdot \bar{m}) \cdot (l \cdot \bar{r})^2$$

where M is the total mass of the subject, $\overline{m}$ is the mean percentage of (mono) segment mass, l is the (mono) segment length and $\bar{r}$ is the mean radius of gyration about the corresponding axis.

Now, for further segmenting the foot model, the decision was to use a scaling factor (sf) for each segment depending on its moment of inertia, as follows:

$$sf = \frac{segment\ mass \cdot segment\ length^2}{foot\ mass \cdot foot\ length^2}$$

So, as a result, for each segment, the moments of inertia will be calculated as:

$$I_k(segment) = sf \cdot I_k(total)$$

where k refers to the axis about which we want to calculate the given moment.

With regard to the inertia tensor, as previously happened with the center of gravity, the only one we are truly interested in is the Forefoot's:

$$\mathbf{I}\,(FF) = 10^{-3} \cdot \begin{bmatrix} 0.3575 & 0 & 0 \\ 0 & 0.3249 & 0 \\ 0 & 0 & 0.0832 \end{bmatrix}$$

Rotation Matrix for each segment

Since we will be using Euler Parameters for spatial orientation, we will need the expression of the Rotation Matrix using these parameters, which has the following structure:

$$\mathbf{A}\,(\text{segment}_i, \text{t}_k) = \begin{bmatrix} 1 - 2 \cdot e_2^2 - 2 \cdot e_3^2 & 2 \cdot (e_1 \cdot e_2 - e_0 \cdot e_3) & 2 \cdot (e_1 \cdot e_3 + e_0 \cdot e_2) \\ 2 \cdot (e_1 \cdot e_2 + e_0 \cdot e_3) & 1 - 2 \cdot e_1^2 - 2 \cdot e_3^2 & 2 \cdot (e_2 \cdot e_3 - e_0 \cdot e_1) \\ 2 \cdot (e_1 \cdot e_3 - e_0 \cdot e_2) & 2 \cdot (e_2 \cdot e_3 + e_0 \cdot e_1) & 1 - 2 \cdot e_1^2 - 2 \cdot e_2^2 \end{bmatrix}$$

(Nikravesh, P. E., 1988)

where segment_i refers to any of the two segments after the Hallux segment simplification (FF, HF) and t_k refers to any k instant of time between Heel Rise and takeoff.

This rotation matrix will allow us to obtain any vector that is in expressed in the local coordinate system of any of the segments in the global coordinate system simply by pre-multiplying it by this matrix; similarly, the opposite will be possible by simply using the inverse of this rotation matrix in the same fashion.

Lastly, to change the expression of any given vector between two local reference systems, we will only have to pre-multiply it by two consecutive rotation matrices: first, the inverted matrix of the new local system and second, the one of the previous system.

Calculation of $\boldsymbol{\omega_i}$, $\boldsymbol{\alpha_i}$ $\boldsymbol{\bar{\omega}_i}$, $\boldsymbol{\bar{\alpha}_i}$, $\boldsymbol{v_i^O}$, $\boldsymbol{a_i^O}$

For the calculation of $\boldsymbol{\omega_i}$, $\boldsymbol{\alpha_i}$, $\boldsymbol{\bar{\omega}_i}$ and $\boldsymbol{\bar{\alpha}_i}$, we will use one of two matrices to relate angular velocity or angular acceleration to the first or second time-derivatives of the Euler Parameters' array, which are:

$$\mathbf{L}\ (segment_i, t_k) = \begin{bmatrix} -e_1 & e_0 & e_3 & -e_2 \\ -e_2 & -e_3 & e_0 & e_1 \\ -e_3 & e_2 & -e_1 & e_0 \end{bmatrix}$$

$$\mathbf{G}\ (segment_i, t_k) = \begin{bmatrix} -e_1 & e_0 & -e_3 & e_2 \\ -e_2 & e_3 & e_0 & -e_1 \\ -e_3 & -e_2 & e_1 & e_0 \end{bmatrix}$$

where **L** and **G** are the initials of Local, Global to relate angular velocity and acceleration in local or global reference systems to the Euler Parameter's time-derivatives, using the following expressions:

$$\boldsymbol{\omega_i} = 2 \cdot \mathbf{G_i} \cdot \dot{\boldsymbol{\theta}}_\mathbf{i}$$

$$\boldsymbol{\bar{\omega}_i} = 2 \cdot \mathbf{L_i} \cdot \dot{\boldsymbol{\theta}}_\mathbf{i}$$

$$\boldsymbol{\alpha_i} = 2 \cdot \mathbf{G_i} \cdot \ddot{\boldsymbol{\theta}}_\mathbf{i}$$

$$\boldsymbol{\bar{\alpha}_i} = 2 \cdot \mathbf{L_i} \cdot \ddot{\boldsymbol{\theta}}_\mathbf{i}$$

For the two other variables, $\mathbf{v_i^O}$ and $\mathbf{a_i^O}$, all we have to do is calculate the first and second time-derivatives, respectively, of the position vector of each segment's origin.

Calculation of $\boldsymbol{a_i^G}$

Once we have calculated all of the previous variables, obtaining $\mathbf{a_i^G}$ is just a matter of employing the following expression to relate them:

$$\mathbf{a_i^G} = \mathbf{a_i^O} + \boldsymbol{\alpha_i} \wedge \overline{\mathbf{OG_i}} + \boldsymbol{\omega_i} \wedge (\boldsymbol{\omega_i} \wedge \overline{\mathbf{OG_i}})$$

where $\overline{\mathbf{OG}}$ can be expressed as:

$$\overline{\mathbf{OG_i}} = \mathbf{A_i} \cdot \overline{\mathbf{cog_i}}$$

where $\overline{\mathbf{cog_i}}$ is the position vector of the center of gravity of segment *i* with respect to the origin of that same segment, in its local coordinate system.

Actions involved

In general, for any given segment, the forces that will play a role will be the following:

- Gravitational forces
- Inter-segment forces
- GRF forces

Similarly, the moments will include:

- Inter-segment moments
- Inter-segment force-derived moments
- GRF moments
- GRF force derived moments

Formulation of the problem

The force balance equation will be expressed using the global reference system, whereas the moment balance equation will be expressed in the Forefoot's local reference system.

The reasons for the second decision are the following:

- In the local coordinate system, since it is fixed with respect to the segment, the inertia tensor will be constant in time.
- In the local coordinate system, since it is fixed with respect to the segment, the inertia tensor will only have elements in its diagonal.

For every segment we will be using two three-dimensional vector equations, one as a force balance ($\sum_k \mathbf{F_k} = m_i \cdot \mathbf{a_i^G}$) and the other as a moment balance ($\sum_k \mathbf{M_k} = \mathbf{I_i} \cdot \boldsymbol{\alpha_i}$), which will

be calculated in the Forefoot's center of gravity; However, since the Hallux segment was removed for simplicity reasons, we will only need the equations of the Forefoot segment:

$$\mathbf{F_{HF-FF}} + \mathbf{F_{grav}} + \mathbf{F_{GRF}} = m_{FF} \cdot \mathbf{a_{FF}^{G}}$$

$$\mathbf{M_{HF-FF}} + \mathbf{F_{HF-FF}} \wedge \mathbf{r_{int-cdgFF}} + \mathbf{M_{GRF}} + \mathbf{F_{GRF}} \wedge \mathbf{r_{GRF-cdgFF}} - \boldsymbol{\omega}_{\mathbf{FF}} \wedge (\mathbf{I_{FF}} \cdot \boldsymbol{\omega}_{\mathbf{FF}}) = \mathbf{I_{FF}} \cdot \boldsymbol{\alpha}_{\mathbf{FF}}$$

where $r_{int-cdgFF}$ is the position vector that goes connects the interface (the "joint" between two segments) between Hindfoot and Forefoot and the center of gravity of the later and $r_{GRF-cdgFF}$ is the position vector that connects the center of gravity of the force plate to the center of gravity of the Forefoot.

Our two only unknowns will be the inter-segment forces and moments between the Hindfoot and the Forefoot ($\mathbf{F_{HF-FF}}$ and $\mathbf{M_{HF-FF}}$), since:

- $\mathbf{F_{grav}} = [0 \;\; 0 \;\; -m_{FF} \cdot g]'$, constant and known
- $\mathbf{F_{GRF}}$ is a piece of information derived from the force plate
- m_{FF} was estimated in section 3
- $\mathbf{a_{FF}^{G}}$ is known as a result of the kinematic calculations explained in section 5
- $\mathbf{r_{int-cdgFF}}$ is derived from the estimation of the Forefoot's segment length, and assuming its center of gravity is at the mid-point of the longitudinal *x* axis
- $\mathbf{M_{GRF}}$ is a piece of information derived from the force plate
- $\mathbf{r_{GRF-cdgFF}}$ is a variable that is completely defined by knowing the position of the GRF's center of gravity (which is stored as a variable as a result of the kinematic analysis) and the position of the Forefoot's center of gravity.
- $\boldsymbol{\omega}_{\mathbf{FF}}$ was calculated in section 5
- $\mathbf{I_{FF}}$ was calculated in section 3
- $\boldsymbol{\alpha}_{\mathbf{FF}}$ was calculated in section 5

Also, the summand $-\boldsymbol{\omega}_{\mathbf{FF}} \wedge (\mathbf{I_{FF}} \cdot \boldsymbol{\omega}_{\mathbf{FF}})$ is part of the second equation because it will be calculated using local coordinates as opposed to a global coordinate system, like is the case in the first equation.

Results

MidFoot Angles

The reference systems used for each one of the results are the following: as far as the MidFoot Internal Moments go, the Hindfoot's local Cartesian system was used; in the case of the angles between the Hindfoot and the Forefoot, relative degrees were employed.

Dorsiflexion and abduction present the greatest of the peak values, with suppination reaching only around half of the magnitude formed in the other two planes.

MidFoot Moments

This is the main focus of the present study. General shapes of the curves were found to be very similar to those presented by Dixon et al. (2012), although peak values for the two first figures (plantarflexion and pronation) were much greater than in the aforementioned case, between a five and a ten-fold increase. Conversely, in the third figure, peak value is close to Dixon's, as is the overall shape if we only take into account the portion starting at 60% of stance phase, which is approximately the value at which Heel Rise occurs in the case of his study.

The most reasonable explanation for such great of a difference in magnitude is the nature of the subjects; in Dixon et al. (2012), individuals were young adolescents (ages around 14 years of age), with a body weight of approximately 53 kg, whereas in the present study, the subject is a 33 year old adult, with a weight of 73 kg.

The general progression of the plantarflexion moment is a start in the negative values before Heel Rise, with a change in sign from this point on. This change is very intuitive, given that from a simple observation of the foot's motion one can clearly see this inversion in the bend.

Peak value is found between 70 and 80% of stance phase, reaching around 1,000 N·mm. At 100% of this phase, after the toe's takeoff, there is no more bending moment in this direction of the foot.

In the case of the pronation, just like in the findings of Dixon et al. (2012), the initial slope (at around Heel Rise) is of a much lesser value than in the previous case. Similarly, peak magnitude only reaches around 650 N·mm, and at around the same point, approximately at 75% of stance. Even though this value is also much greater than in the case of reference, it is true that the proportion between the two respective figures in both trials is constant, which would seem reasonable if the sole difference between the studies were the subjects used.

MidFoot Power Generation

Given the difference between the moments results presented by Dixon et al. (2012), and those in this document, one would also expect power to be between five and ten times greater than in the former case; however, it is only between two and four times greater. If this were

true, it would mean that angular velocity in the adult subject is slower than in the young adolescents.

As far as the shape goes, it is identical to its analogous in Dixon's paper: peak value reached at around 85 to 90% of the stance phase, and a power of around zero up until rather advanced stages in this phase, finishing at zero a little bit before the takeoff of the Hallux.

Relative Importance of each summand of the equation

Throughout the following figures, which represent the summands of the moment's equation in all three axis, we can observe the negligible inertial contribution of the dynamic equations to the overall result. The predominant factor in them is the ground reaction force, in the case of the force equation, and ground reaction moment and moment derived from force in the moments equation.

In the moments equation (which are the results presented in these three figures), there is a smaller but very significant contribution of the moment caused by the midfoot's inner forces, which are no more than a mere result of the balance between forces, where the ground reaction force is predominant.

3. CONCLUSIONS

After analyzing these results and comparing them to those presented by Dixon et al. (2012), the following conclusions can be extracted:

- In the present study, an adult subject was in charge of gathering the data; a 40% increase in his weight with respect to the young adolescents in the aforementioned paper could explain the difference in two of the three magnitudes of the moments, with the shape being very similar in all cases.

- Given that this experiment was only conducted on one subject, and only in one occasion, it is possible that some peculiarities out of the ordinary in gait were captured and thus further differentiation in the moments' magnitudes have been made evident, through a prior difference in the relative angles between the segments.

- As a non-linear problem, the possibility of small errors in marker placement (specially as the subject was the one placing his owns markers) may have lead to a big distortion in relative angles between the different segments.

- Lack of information about the GRF distribution has forced to making certain simplifications which may not be ideal; using more advanced technology, such as a device informing of pressure distribution, would aid in this sense. Probably the Hallux segment is more important than presented in this paper, as for instance, in the last fraction of the stance phase, it is the only segment in contact with the floor; however, since it had previously been eliminated, the forces gathered by the force plate were directly applied to the Forefoot.

- A better method for estimating both, the centers of gravity, as well as the moments of inertia of each segment (there was adequate information only for the mono-segment case) would be very useful.